

Pelagic molybdenum concentration anomalies and the impact of sediment resuspension on the molybdenum budget in two tidal systems of the North Sea

Nicole Kowalski^{1*}, Olaf Dellwig¹, Melanie Beck², Ulf Gräwe¹, Nadja Neubert^{3,4}, Thomas F. Nögler³, Thomas H. Badewien², Hans-Jürgen Brumsack², Justus E. E. van Beusekom^{5,6}
& Michael E. Böttcher¹

¹ Leibniz Institute for Baltic Sea Research Warnemünde (IOW), Seestraße 15, D-18119 Rostock, Germany

² Institute for Chemistry and Biology of the Marine Environment (ICBM), Carl von Ossietzky University of Oldenburg, D-26111 Oldenburg, Germany

³ Institute of Geological Sciences, University of Bern, CH-3012 Bern, Switzerland

⁴ Present address: Institute of Mineralogy, Leibniz University of Hannover, Callinstr.3, D-30167 Hannover, Germany

⁵ Alfred Wegener Institute for Polar and Marine Research, Wadden Sea Station Sylt, Hafenstraße 43, D-25992 List, Germany

⁶ Present address: Helmholtz-Zentrum Geesthacht, Institute for Coastal Research, D-21502 Geesthacht, Germany

* Corresponding author, phone: +49(0)381-51 97 361, fax: +49(0)381-51 97 352,
E-mail addresses: nicole.kowalski@io-warnemuende.de; kowalski_nicole@yahoo.de

Abstract

The seasonal dynamics of molybdenum (Mo) were studied in the water column of two tidal basins of the German Wadden Sea (Sylt-Rømø and Spiekeroog) between 2007 and 2011. In contrast to its conservative behaviour in the open ocean, both, losses of more than 50% of the usual concentration level of Mo in seawater and enrichments up to 20% were observed repeatedly in the water column of the study areas. During early summer, Mo removal by adsorption on algae-derived organic matter (e.g. after *Phaeocystis* blooms) is postulated to be a possible mechanism. Mo bound to organic aggregates is likely transferred to the surface sediment where microbial decomposition enriches Mo in the pore water. First $\delta^{98/95}\text{Mo}$ data of the study area disclose residual Mo in the open water column being isotopically heavier than MOMo (Mean Ocean Molybdenum) during a negative Mo concentration anomaly, whereas suspended particulate matter shows distinctly lighter values. Based on field

observations a Mo isotope enrichment factor of $\epsilon = -0.3\text{‰}$ has been determined which was used to argue against sorption on metal oxide surfaces. It is suggested here that isotope fractionation is caused by biological activity and association to organic matter.

Pelagic Mo concentration anomalies exceeding the theoretical salinity-based concentration level, on the other hand, cannot be explained by replenishment via North Sea waters alone and require a supply of excess Mo. Laboratory experiments with natural anoxic tidal flat sediments and modelled sediment displacement during storm events suggest fast and effective Mo release during the resuspension of anoxic sediments in oxic seawater as an important process for a recycling of sedimentary sulphide bound Mo into the water column.

Keywords

Molybdenum, Mo isotopes, *Phaeocystis* sp., sediment resuspension, storm events, tidal flats, German Wadden Sea, North Sea

1. Introduction

Molybdenum (Mo) is a redox-sensitive trace metal occurring as dissolved molybdate (MoO_4^{2-}) in the oxygenated ocean with a concentration of about 110 nM (Morris, 1975; Collier, 1985). Although Mo is involved in biological cycles, its behaviour is generally considered to be conservative (e.g. Howard and Cole, 1985; Cole, 1993). An increasing number of recent studies, however, demonstrate temporal deviations from conservative behaviour in different aquatic ecosystems. Mo removal from oxic seawater can be caused by various processes, e.g., scavenging by freshly formed manganese oxides, Fe-oxyhydroxides, organic matter, and assimilation by phytoplankton (e.g. Szilagyi, 1967; Head and Burton, 1970; Berrang and Grill, 1974; Nissenbaum and Swaine, 1975; Yamazaki and Gohda, 1990; Cole, 1993; Tuit and Ravizza, 2003). Substantial temporary Mo depletion in coastal and offshore waters was first observed by Dellwig et al. (2007) who suggested Mo fixation in oxygen-depleted microzones of aggregated suspended matter and/or adsorption to freshly formed organic matter.

In sulphidic environments MoO_4^{2-} is transformed to particle-reactive thiomolybdates (Erickson and Helz, 2000) until final burial as MoS_2 . Furthermore, Mo can be incorporated into Fe sulphides or bound to organic matter (e.g. Huerta-Diaz and Morse, 1992; Helz et al., 2004; Vorlicek et al., 2004; Helz et al., 2011). In addition, substantial adsorption of Mo on the surfaces of Mn and Fe oxi(hydroxi)des has been found (e.g., Berrang & Grill, 1974) which

may lead to a cycling between the oxic and suboxic zones of aquatic and sedimentary systems when these species are oxidized or reduced.

In permeable sediments influenced by advective pore water transport, Mo attached to metal oxides can be transported into anoxic sediment layers (Boudreau and Jørgensen, 2001; Rusch and Huettel, 2000) and may be released when the metal oxides are reduced by H₂S (Adelson et al., 2001). Complexation by dissolved organic compounds has been suggested to cause stabilisation of dissolved Mo (Brumsack and Gieskes, 1983) which may retard the fixation in anoxic sediments thereby allowing again the release into the overlying water column (Dellwig et al., 2007; Beck et al., 2008; Kowalski et al., 2009).

Mo isotope fractionation is known to occur when Mo is removed from the aqueous solution during fixation by different solid interfaces under anoxic and oxic conditions (e.g., Barling and Anbar, 2004; Arnold et al., 2004; Nägler et al., 2005; Goldberg et al., 2009, 2012). Thus, Mo isotopes are a useful tool to identify the processes involved in Mo partitioning between water column and sediment. While the scavenging of Mo by Mn oxides is suggested to result in light isotope signatures (Barling et al., 2001; Siebert et al., 2003; Poulson et al., 2006; Wasylenki et al., 2008; Goldberg et al., 2012), more effective removal of Mo from solution under euxinic conditions leads to smaller to negligible isotope fractionation depending on the sulphide level (e.g. McManus et al., 2002; Arnold et al., 2004; Neubert et al., 2008; Nägler et al., 2011).

Reoxidation of sedimentary sulphidic compounds may take place during e.g. extensive sediment displacement (Aller et al., 1986) or bioturbation (Boudreau and Jørgensen, 2001; Volkenborn et al., 2007) and may result in a significant release of trace metals like Mo. A partial reoxidation can be also caused by advective circulation of oxygenated waters through the top sediments which enhances O₂ penetration into permeable sediments (de Beer et al., 2005).

Large scale sediment erosion and resuspension of tidal flat sediments is caused by tide- and wind-driven wave activity (e.g. de Jonge and van Beusekom, 1995; You, 2005; Stanev et al., 2006; Christiansen et al., 2006; Bartholomä et al., 2009; Fettweis et al., 2007, 2010). Pronounced sediment transport may in particular take place during storm events. Such resuspension processes also cause remobilisation and transfer of trace metals into the water column (e.g., Cantwell et al., 2002; Saulnier and Mucci, 2000; Audry et al., 2006, 2007; Kalnejais et al., 2007, 2010) finally altering the geochemical signature of the open water column. The extent of the impact will depend on the reservoir sizes and the residence time of sedimentary compounds under oxic conditions (Morse, 1994; Saulnier and Mucci, 2000).

With the help of modelling approaches, the residence times and fluxes of suspended particulate matter in the water column during storm conditions can be estimated (e.g. Warner et al., 2008; Lettmann et al., 2009; Gräwe and Wolff, 2010; Dobrynin et al., 2010).

In this contribution, we investigate the seasonal dynamics of Mo in two tidal systems of the German Wadden Sea with different sedimentological and hydrodynamic properties. Possible mechanisms for non-conservative behaviour of Mo as expressed by temporary negative and positive concentration anomalies in the water column are discussed. In this context, the oxidative release of Mo from the sediments during resuspension is examined by experimental and modelling approaches estimating the potential consequences for the Mo inventory in the water column. Furthermore, we present first Mo isotope data from the coastal area of the North Sea, which provide complementary information about the geochemical behaviour of Mo.

2. Study areas

The Wadden Sea is about 450 km long stretching from Den Helder in the Netherlands to Blåvandshuk in Denmark along the southern North Sea coastline (Streif, 1990). Sampling was carried out in the backbarrier tidal flats of the Islands of Spiekeroog in the southern part of the German Wadden Sea and in the backbarrier tidal flats of the Islands Sylt and Rømø in the northern part (Fig. 1).

The backbarrier tidal area of Spiekeroog Island (Fig. 1A) covers an area of about 74 km² (Walther, 1972) and water exchange with the open North Sea occurs via the tidal inlet (Otzumer Balje, OB) between the Islands of Langeoog and Spiekeroog. Tides are semi-diurnal with a mean range of 2.6 m (Flemming and Davis, 1994). The backbarrier area is dominated by sand and mixed flat sediments with grain sizes decreasing towards the mainland due to lower current velocities (e.g. Postma, 1961; Reineck et al., 1986; Flemming and Nyandwi, 1994).

The Sylt-Rømø tidal basin (Fig. 1B) is a semi-enclosed bight encompassing an area of about 407 km² and is characterised by semi-diurnal tides with a mean range of about 2 m. Tidal water transport occurs via a single tidal inlet branching into three main tidal channels (Gätje and Reise, 1998). Most of the sediment consists of mixed sand and sandy sediments whilst fine sediments prevail along the fringes (Bayerl et al., 1998).

3. Material and Methods

3.1. Sampling

Water and suspended particulate matter (SPM) samples were taken aboard R/V “Navicula” close to a time series station in the tidal inlet of site Spiekeroog (site OB, Fig. 1A, 53°45.0'N, 7°40.3'E; water depth ca. 13 metres, Grunwald et al., 2007). At Sylt Site, sampling was carried out in the tidal channel called Lister Ley (LL, Fig. 1B, 55°01.30' N, 8°27.10' E, water depth ca. 10 metres) using R/V “Mya”.

For SPM, 0.5 to 1 L seawater was filtered through pre-weighted polycarbonate filters (Millipore Isopore membrane filters, 0.4 µm pore size, low-pressure max -20 kPa). Afterwards the filters were rinsed with 100 mL purified water and dried for 48 h at 60° C. For algae cells counts, water samples were fixed with Lugols solution and stored in amber glass bottles at 4°C.

Seawater samples were filtered through 0.45 µm SFCA (surfactant-free cellulose acetate) syringe filters and acidified to 1% (v/v) with concentrated HNO₃ (supra pure, Merck).

Surface sediment samples were taken with cut plastic 60 ccm syringes, placed into 60 ccm plastic centrifuge tubes, and, after return to the laboratory, kept frozen until freeze-drying and further analysis as described by Neubert et al. (2008).

3.2. Analytical methods

At site Spiekeroog, temperature was determined as a mean of ten minutes intervals at the time series station (OB). Salinity was calculated from temperature, conductivity and hydrostatic pressure (UNESCO, 1985). In the Sylt area, temperature was measured with an electronic reversing thermometer (SiS, Sensoren Instrumente Systeme GmbH) which was mounted on a niskin bottle. Salinity was measured with a salinometer (Guildline Instruments, Autosal 8400).

For analysis of Mo in suspended particulate matter (SPM) the polycarbonate filters were digested with a mixture of HNO₃, HClO₄, and HF using a pressure digestion system PDS-6 (Loftfields Analytical Solutions; Heinrichs et al., 1986) at 180°C for 6h and were measured by ICP-OES (Thermo, iCAP 6300 Duo). A detailed description of the digestion method, which was also used for sediment samples, is given by Dellwig et al. (2007). Accuracy and precision of the analyses were determined by simultaneous measurements of the certified reference standard SGR-1 (green river shale, United States Geological Survey) and were better than 7.3% and 5.6%, respectively.

Dissolved Mo and Mn in seawater samples were measured by ICP-OES (Thermo, iCAP 6300 Duo) and HR-ICP-MS (Element II, Thermo Fisher Scientific) using 2-fold and 10-fold diluted aliquots, respectively. Accuracy and precision were determined with the certified seawater standard CASS-4 (National Research Council of Canada) and were better than 7.5% and 6.5%, respectively.

Taxa determination and cell counting was performed using an inverted microscope following the Utermöhl method (Utermöhl 1931, Lund et al. 1958). Phytoplankton cell dimensions were measured for up to 25 cells of every taxon that occurred at the respective sampling date. Cell volumes were calculated according to the geometric shapes proposed by Hillebrand et al. (1999).

For $\delta^{98/95}\text{Mo}$ measurements 100 ml water were spiked with a ^{97}Mo and ^{100}Mo double-spike. After evaporation, the samples were redissolved in 4 M HCL with trace H_2O_2 . Mo purification applying anion and cation exchange columns followed Neubert et al. (2011). The isotopic composition of Mo was measured with a Nu instruments MC-ICP-MS. A detailed description of the analytical technique is given by Siebert et al. (2001) and Wille et al. (2007). A minimum of 20 ng Mo was used per analyses. Analytical blanks (<2 ng) were small compared to the typical total amount of sample Mo processed (<1.5%). For isotope data presentation the $^{98}\text{Mo}/^{95}\text{Mo}$ ratio was used. The standard reproducibility was better than 0.06‰ (2 σ). Isotope composition was presented as ‰ deviation from Johnson Matthey ICP standard solution (lot 602332B, Siebert et al., 2001):

$$\delta^{98/95}\text{Mo} = [(^{98}\text{Mo}/^{95}\text{Mo})_{\text{sample}} / (^{98}\text{Mo}/^{95}\text{Mo})_{\text{standard}} - 1] * 10^3 \quad [1].$$

The $\delta^{98/95}\text{Mo}$ of NIST SRM 3134 is 0.25‰ relative to this standard, and ocean water (Mean Ocean Molybdenum, MOMo) is 2.34 ± 0.07 ‰ (Greber et al 2012).

3.3. Oxidation experiment

A laboratory experiment with natural anoxic tidal flat sediments was conducted to investigate the liberation of Mo during mixing with oxygenated seawater. After removal of the thin oxic surface layer (1-5 mm), the first 10 cm of anoxic sediment material were collected in March 2008 from a sand flat (Fig. 1A, Janssand JS, 53°44.18' N, 7°41.90' E, mud fraction <5%) and a mixed flat site (Fig. 1A, NN, Neuharlingersieler Nacken, 53°42.15' N, 7°42.57' E, mud fraction about 15%) to consider the dominant sediment types of the study area (e.g., Flemming and Ziegler, 1995; Al-Raei et al., 2009). In the laboratory, the sediments

were sub-sampled in a glove bag under N₂ atmosphere (Sigma-Aldrich, Milwaukee, USA) to avoid O₂ contamination. For metal analysis of the original material, samples were taken from both sediment types and stored frozen in plastic petri dishes until analyses. For the experiment about 1 kg of the sediment material was filled into plexiglass tubes (length 45 cm, diameter 5 cm) closed with rubber plugs. The experiment started with the addition of 0.5 L oxygenated artificial sea water containing no Mo. The tubes were agitated continuously during the entire experiment duration of 6 h using a shaking bed (Gerhardt Analytical systems, Königswinter, Germany) to ensure homogenous resuspension of the sediment material. Aliquots of 2 mL were taken from the water column every 15 min with a 5 mL syringe for the analysis of dissolved Mo released during oxidation. Based on pore water Mo concentrations and the water content of the used sediment, a possible interference of pore water Mo can be excluded. Immediately after sampling the aliquots were filtered through 0.45 µm SFCA syringe filters and acidified to 1% (v/v) with concentrated HNO₃. The solutions were analysed by ICP-OES as described above.

3.4. Estimating SPM residence times with a Lagrangian particle tracking model

A Lagrangian particle tracking model (Gräwe and Wolff, 2010) was used to simulate short-term SPM dynamics and particle residence time in the water column of the backbarrier area of Spiekeroog Island using the conditions during the storm event “Britta” (31 October - 2 November 2006). On that account, the Lagrangian SPM module was adapted to a hydrodynamic core model (GETM, General Estuarine Transport Model, Burchard and Bolding, 2002) which was coupled to a wave model (SWAN, Simulating Waves Nearshore, Booij et al., 1999). A detailed description and validation of the hydrodynamic model and the Lagrangian particle tracking model can be found in Lettmann et al. (2009) and Gräwe and Wolff (2010).

The model simulated the time period from 20 October to 4 November 2006. To estimate the residence time of particles in the water column the following procedure was used: 1500 particles with a diameter of 50 µm were placed randomly distributed in each 200 x 200 m grid cell (20 million particles in total). The diameter was chosen as a fair estimate for the present grain size spectrum ranging from clayey to sandy material. As soon as the bottom stress of 0.12 N/m² was reached, particles could be resuspended and released into the water column. For bottom stress values below 0.12 N/m² only sedimentation was possible. For a detailed description and validation of the erosion and sedimentation modules the reader is referred to Gräwe and Wolff (2010).

For each particle, the residence time in the water column, i.e., the time from resuspension until deposition, was calculated. Afterwards, a mean value was calculated for all particles in a grid box. This procedure was done over one tidal cycle computing a temporal average over these 12.4 hours (this limits the maximum residence time to 12.4 hours). Thereafter, the particle positions were reset and the simulation was started again with a time shift of 2 hours until the final simulation time was reached.

4. Results and discussion

4.1. Negative concentration anomalies of dissolved Mo

Distinct deviations of dissolved molybdenum (Mo_{diss}) from salinity-based theoretical values appeared repeatedly in the water column of Site Spiekeroog (OB) during certain time periods between 2007 and 2010 (Fig. 2a). In comparison to previous studies (Dellwig et al., 2007; Kowalski et al., 2009), the time-series presented in this contribution revealed significant fluctuations of Mo_{diss} throughout the years due to a higher sampling resolution over an extended time period. During early summer Mo_{diss} decreased temporarily down to a minimum value of 50 nM representing less than 50% of the salinity-based Mo concentration. Unfortunately, this behaviour could not be shown in 2009 due to lacking samples for the time period between mid-June until the end of August. The negative Mo_{diss} concentration anomaly was also observed at the Sylt Site in 2008, less pronounced in 2010, and again in 2011 (Fig. 3a). This observation allows the conclusion, that Mo depletions are common phenomena in the investigated tidal basins of the North Sea, thus likely appearing within the entire Wadden Sea. The decrease in Mo_{diss} concentrations at the Sylt Site was observed in the years 2008-2010 about four weeks later than at the Spiekeroog Site. This is in line with previous observations (Dellwig et al., 2007) which indicated a development of the Mo_{diss} concentration anomaly from the western to the eastern parts of the East Frisian Wadden Sea.

Several authors reported coupled transport behaviour between Mo and Mn via scavenging of Mo by Mn oxides (e. g., Berrang and Grill, 1974). The time-series of site Spiekeroog in 2007 and 2008 revealed a parallel decrease of Mo_{diss} and Mn_{diss} concentrations which may be a result of elevated photochemical and/or bacterial Mn oxidation (Emerson et al., 1982; Anbar and Holland, 1992; Nico et al., 2002) and subsequent scavenging of Mo. However, observations by Dellwig et al. (2007) and Kowalski et al. (2012) showed that the decreasing Mn_{diss} concentrations in summer were not caused by Mn oxidation but were due to decreasing availability of reactive Mn in the surface sediments.

A comparison with the phytoplankton dynamics (Figures 2b and 3b) implied a connection between the Mo_{diss} depletion and phytoplankton blooms (expressed as cell carbon) in early summer. Although the diatom blooms in spring seemed to have a limited influence on the Mo_{diss} concentrations, pronounced depletions occurred after the *Phaeocystis* blooms. This early summer depletion persisted for the longest period at the Spiekeroog Site in 2008. A significant loss of Mo_{diss} is seen in June followed by a second smaller decline in August which may be attributed to the influence of the *Phaeocystis* bloom in April/May and the less pronounced summer diatom bloom in June/July. At the Sylt Site, the diatom bloom occurred about one month later at the end of March 2008 (Figs. 3b). Similar to the diatoms, *Phaeocystis* sp. also bloomed later in Sylt, which was followed by a significant negative concentration anomaly of Mo_{diss} . These differences in timing of the blooms were probably related to local factors including temperature (e.g. van Beusekom et al., 2009) and light conditions during the previous winter months (e.g. Cadée, 1986). The shorter duration of the Mo depletion near Sylt might be due to the less pronounced *Phaeocystis* bloom ($390 \mu\text{g carbon L}^{-1}$). The importance of the *Phaeocystis* bloom in early summer became especially clear in the time series data of Sylt Site in 2010. Although the diatom bloom in spring lead to exceptionally high cell carbon concentrations, the Mo_{diss} depletion was only weakly expressed as *Phaeocystis* sp. also showed only low abundance. However, the lacking Mo depletion at Sylt Site in 2009, albeit a pronounced *Phaeocystis* bloom was present, remains enigmatic.

The crucial difference between diatom and *Phaeocystis* blooms is the enormous release of organic mucus during breakdown of the latter species (e.g. Schoemann et al., 2005). Although the mucilaginous matrix is not included in the determined cell carbon (Figs. 2b and 3b) a considerable release of excess organic matter to the water column can be assumed which probably traps Mo_{diss} . This assumption is supported by measurements of suspended particulate matter during a Mo depletion period in July 2005 when organic matter contents (max. 29%) corresponded with elevated Mo values (max. 40 mg kg^{-1}) (Dellwig et al., 2007). Furthermore, the proposed relationship between Mo and organic matter is in accordance with a number of studies (Szilagyi, 1967; Head and Burton, 1970; Nissenbaum and Swaine, 1975; Yamazaki and Gohda, 1990; Coveney et al., 1991; Helz et al., 1996; Lyons et al., 2003; Algeo et al., 2007).

The transfer of Mo_{diss} onto SPM was also indicated by $\delta^{98/95}\text{Mo}$ values showing an enrichment of the lighter isotope on SPM whereas the residual Mo_{diss} fraction revealed a heavier isotopic composition finally pointing towards isotopic fractionation and preferential removal of the lighter Mo isotope from the aqueous phase (Table 1, Fig. 4). The net non-

conservative behaviour of dissolved Mo suggests that in a first-order approach the water column can be regarded as a closed system with respect to Mo_{diss} . Therefore, based on the development of the aqueous solution, an enrichment factor was calculated considering a Rayleigh approach:

$$\varepsilon = (\delta^{98/95}\text{Mo} - \delta^{98/95}\text{Mo}_{\text{MOMo}}) / \ln f \quad [2]$$

$$\delta^{98/95}\text{Mo} = \delta^{98/95}\text{Mo}_{\text{MOMo}} + \varepsilon \cdot \ln f \quad [3]$$

with f representing the residual fraction of Mo_{diss} in the water column. Evaluation of the field data yields an enrichment factor ε of -0.3‰ (Fig. 5). Isotope enrichment factors describing the behaviour of Mo isotopes during the interaction between Mo_{diss} and Mn oxides or Fe-oxyhydroxides as well as during the assimilation by microorganisms (soil bacteria, cyanobacteria) have already been established experimentally (Wasylenki et al., 2008; Goldberg et al., 2009; Zerkle et al., 2011). The application of equation (3) using the experimentally derived enrichment factors indicates, that the observed field data cannot be reproduced assuming sorption onto metal (oxyhydr)oxide surfaces as responsible process (Fig. 5). Moreover, the calculated enrichment factor was close to results determined experimentally during active Mo uptake by cyanobacteria (Zerkle et al., 2011). Although cyanobacteria may be important in the sediments of the study area (Evrard et al., 2008), they are not expected to influence the Mo reservoir in the open water column due to negligible abundances and dissolved sulphate at seawater level competing with molybdate for active assimilative uptake (Howarth and Cole, 1985; Cole et al., 1993; Marino et al., 2003). Furthermore, Mo depletion occurred during periods of decreasing phytoplankton abundance and not during the growth period (Fig. 2). Thus, active uptake of Mo by phytoplankton can be ruled out to cause significant Mo_{diss} depletion in early summer. Therefore, it is hypothesised that extracellular Mo-binding to algae-derived organic matter may have caused the observed Mo isotope fractionation, although the actual isotope enrichment factor for Mo adsorption onto organic matter is not known so-far. A more detailed analysis of the processes leading to the observed Mo isotope fractionation effects requires further field and in particular further experimental and modelling studies.

Several studies document adsorption of metal cations onto algal and bacterial cell walls (e.g. Gonçalves et al., 1987; Xue et al., 1988; Fein et al., 1997; Daughney et al., 1998; Seders and Fein, 2011). For instance, Mn is known to be adsorbed to *Phaeocystis* mucus (Davidson

and Marchant, 1987; Schoemann et al., 2005). Phytoplankton releases surface-active exopolymeric substances, supporting the aggregation of organic and inorganic particles (e.g. Passow, 2002a). The increased release of organic matter during and after the breakdown of *Phaeocystis* blooms together with higher water temperatures leads to enhanced microbial activity in early summer (Lemke et al., 2010). The additional release of exudates by bacteria as well as the bacterial modification of phytoplankton-derived substances to transparent exopolymer particles (TEP) by bacteria (Passow, 2002b; Bhaskar et al., 2005) leads to the formation of large aggregates and thus an enhanced flux of organic-rich particles to the sediment surface in the summer months (Riebesell, 1991a, b; Kiørboe et al., 1994; Logan et al., 1995; Simon et al., 2002; Chang et al., 2006; Lunau et al., 2006). Harvey and Leckie (1985) studied the importance of extracellular polysaccharides (EPS) for metal adsorption and found that EPS released by bacteria competes with bacteria cell walls for available metals. Acharya et al. (2009) found anionic uranyl (UO_2^{2+}) being bound to EPS of a marine cyanobacterium. Although less is known about the adsorption of anions (e.g., Fein et al., 2001), Mo_{diss} adsorption to surface-active TEP directly released by *Phaeocystis* sp. as well as organic compounds produced after their blooms is postulated to play a key function in removing Mo_{diss} from the water column in the study area. Such sequence of organic matter production by algae followed by bacterial modification may also explain the time gap between *Phaeocystis* breakdown and Mo depletion (Figs. 2 and 3). In contrast, the less pronounced response of Mo_{diss} dynamics during spring diatom blooms is probably explained by a lower release of organic matter by these species as well as a reduced microbial activity due to lower temperatures (Lemke et al., 2010).

Subsequent aggregation of suspended particles by released organic matter may lead to deposition of organically bound Mo in the sediment (Dellwig et al., 2007). The relatively short time necessary to produce Mo concentration anomalies may be explained by a rapid, event-like sinking and deposition of the large aggregates as it has been reported by e.g. Riebesell (1991a), Alldredge and Gotschalk (1989), and Chang et al. (2006). The transfer of Mo to the surface sediments as well as its release after the decomposition of deposited organic-rich particles is indicated by enrichments of Mo_{diss} in the shallow pore waters of site Spiekeroog partly exceeding the usual seawater value by a factor of four (Dellwig et al., 2007; Beck et al., 2008; Kowalski et al., 2009).

Additionally, the analysis of the periostraca (protective organic coatings) of bivalves found in the sediments of the study area supported the assumption of a tight relation between Mo and organic matter under natural conditions in this environment. While Mo_{part} contents of

the periostracum of *Mytilus edulis* living in colonies above the sediment surface showed values of up to 8 mg kg⁻¹, the burrowing *Ensis americanus* reached contents of up to 256 mg kg⁻¹. The isotopic composition of the latter periostracum resembled those of SPM with a $\delta^{98/95}\text{Mo}$ value of +1.3 ‰ (Table 1) thereby indicating a Mo isotope fractionation between dissolved and organically bound Mo and an enrichment of the lighter isotope in the organic matrix compared to the aqueous solution.

4.2. Positive concentration anomalies of dissolved Mo

Apart from depletion periods, the time series of pelagic Mo_{diss} at both sites also revealed positive Mo concentration anomalies. While the time-series of Mo_{diss} generally showed a slightly enhanced level at Spiekeroog Site in 2009 and at Sylt Site in 2011 most prominent anomalies occurred especially in late summer 2007, 2010 and spring 2008 at Spiekeroog Site and early summer 2009 as well as spring 2011 at Sylt Site. The enrichments were about 20 nM above the theoretical salinity-based Mo_{diss} values (Mo_{sal}; Figs 2a and 3a) and thus significantly above the analytical error (compare Chapter 3.2). Enhanced Mo_{diss} concentrations in spring may be caused by the release of Mo_{diss} during the reduction of Mn oxides in the surface sediments when anoxic conditions reach the uppermost sediment layer (Burdige and Nealson, 1985). However, the water column data from both sites did not clearly support a direct relation between Mo_{diss} and Mn_{diss} dynamics within the study area (Figs. 2a and 3a). Although a certain relation might be inferred from slightly increasing Mo_{diss} values in spring at Spiekeroog Site, distinctly lower Mn_{diss} enrichments at Sylt Site argue against a significant release of Mo due to the reduction of Mn oxides in the surface sediments. This is also true for reduction of Fe-oxihydroxides as seen in pore water profiles from Spiekeroog Site showing no relation between Fe and Mo dynamics (Kowalski et al., 2009). Assuming a comparable Mo content of the sedimentary Mn oxides at both sites, the about four-times higher Mn maxima at Spiekeroog, e.g. in spring 2008 and 2009, should lead to much more pronounced positive concentration anomalies.

High concentrations after depletion periods at the Spiekeroog Site may be due to Mo_{diss} release from the sediments into the overlying water column after the occurrence of high Mo_{diss} enrichments in the pore waters (Dellwig et al. 2007; Kowalski et al., 2009). Furthermore, sediment resuspension due to wind-induced wave action and tidal currents during tidal drainage and inundation (Roman and Tenore, 1978; Lavelle et al., 1984; de Jonge and van Beusekom, 1995; Christiansen et al., 2004, 2006; Sterckx et al., 2007; Bartholomä et al., 2009) may contribute to Mo inventories. Intense sediment displacement and transport

influencing biogeochemical element budgets have been reported especially during storm events (e.g. You, 2005; Grunwald et al., 2009; Bartholomä et al., 2009; Kolditz et al., 2012). Busch et al. (1998) observed a clear seasonality of strong wind and storm events occurring mainly in autumn and winter months. As shown in Figure 6a, even wind speeds of about 12 m s⁻¹ (6 bft) were able to increase SPM concentrations significantly. As the permanently oxidised sediment layer is only a couple of millimetres thick during the summer months (Jansen et al., 2009) and local areas with reduced sediment surfaces, so called “black spots”, may occur (Böttcher et al., 1998; Böttcher 2003), resuspension may transfer reduced sediment components as iron-monosulphides (FeS) and associated trace elements like Mo into the oxic water column (Fig. 6b).

An oxidation experiment with natural anoxic sand and mixed flat sediments was carried out to estimate the amount and rate of Mo potentially released during sediment resuspension. The results showed a rapid Mo_{diss} release from the sediments within the first hour reaching maximum values of 0.75 µM for the sand and 4 µM for the mixed flat sediment (Fig. 7a). Further differences between the sediment types were visible in the rates of Mo_{diss} release (Fig. 7b). In the initial phase of the experiment (>15 min) around 0.1 g m⁻³ h⁻¹ more Mo was released from the sand than from the mixed flat sediment. The decrease in oxidation rate and the different steady-state levels were due to differences in the Mo pool sizes and the initial reactive particle surfaces. The isotopic composition of the released Mo_{diss} (Fig. 7c) matched the sedimentary isotope data (Table 1). Although Mo isotope data for Mo_{diss} in the water column during positive Mo concentration anomalies are not available, these results suggest an intense release of isotopically light Mo from the sediments to the water column possibly also causing a shift to a lighter isotopic composition of the water column. Table 1 compares the Mo contents and isotopic composition of sandy surface sediments (from site JS) with typical oxidised surfaces with those which were reduced and coloured black by iron sulphides. The latter should be in particular sensitive to modifications upon storm- or current-induced resuspension. Compared to the oxidised surfaces they are slightly higher enriched in the contents of total Mo and the heavy stable Mo isotope, likely due to a slightly higher fixation of Mo from pore waters under sulphidic conditions.

Figure 8 shows results of a model simulation estimating residence times of mud particles (diameter 50 µm) in the water column over a tidal cycle during calm conditions (Fig. 8a) and the storm event “Britta” from 31 October to 2 November 2006 (Fig. 8b) as well as the difference between both situations (Fig. 8c). During calm conditions, highest residence times due to elevated current velocities were generally seen in the main tidal channel reaching more

than 10 hours (Fig. 8a). At the tidal flat margins particles were still suspended around 5-7 hours while on the tidal flats suspension was shortest (<2 hrs) due to a lower water level (<2m) and less tidal activity.

During the storm event, high erosion and particle resuspension occurred at the northern coasts of the barrier islands due to elevated wave energy (Fig. 8b). On the sand flats within the backbarrier area resuspension was also enhanced (2-4 hrs, Fig. 8c) as the winds from north-westerly direction (Bartholomä et al., 2009) pushed the water masses into the backbarrier area against the ebb current thereby extending duration of water coverage on the tidal flats.

Essential sediment erosion down to 16 cm sediment depth was observed during a storm event in the backbarrier area of Spiekeroog Island by Tilch (2003). This area is even subjected to pronounced sediment displacement under normal conditions as indicated by own observations revealing maximum erosion of about 8 cm in April 2008 and still about 5 cm in summer during wind speeds reaching only up to 16 m s^{-1} (data not shown).

Based on the experimental Mo release rates and the particle tracking model a rough calculation was made to elucidate the potential impact of resuspension on the Mo budget in the open water column. To assure conformity with sediment-water ratio in the study area, which was approximated to 0.08 (74 km² area, Walther, 1972; $145 \times 10^6 \text{ m}^3$ water volume, Lübben et al., 2009; assumed sediment depth of 1 cm = $1.1 \times 10^9 \text{ kg}$ sediment and $145 \times 10^9 \text{ L}$ seawater) the experimental results (Fig. 8a; sediment-water ratio = 2) were adjusted with a factor 0.04 (sediment-water ratio study area / sediment-water ratio experimental setup). When considering a homogenous sediment erosion of 5 cm depth (1 cm oxic zone + 4 cm anoxic sediment) and a sediment distribution of 62% sand flat and 38% mixed/mud flat in the back barrier area of Spiekeroog Island (Al-Raei et al., 2009), $2.8 \times 10^9 \text{ kg}$ anoxic sand and $1.4 \times 10^9 \text{ kg}$ anoxic mixed/mud flat sediments may be suspended in the water column. Assuming a mean residence time of the sediment particles within the oxic water column of two hours, the Mo_{diss} level may be increased by about 25 nM. Thus, in addition to Mo release from deposited organic-rich particles, resuspension is able to considerably affect the pelagic Mo budget and most likely represents an important mechanism contributing Mo to the open water column.

5. Conclusions and outlook

Temporary Mo depletions of 50% of the usual level were found repeatedly in the water column of the German Wadden Sea in early summer between 2007 and 2011, thus representing a typical feature of this ecosystem. The major processes influencing the Mo

cycle in the investigated coastal system are summarized in Fig. 9. As Mo depletions often appeared during/after breakdown of algae blooms, a coupling to algae-derived organic matter is feasible. Especially during the summer months, *Phaeocystis*-derived organic mucus is probably able to trap significant amounts of dissolved Mo which is subsequently transferred to the surface sediment after aggregation of particles and organic matter. Associated Mo isotope fractionation of dissolved Mo during a negative Mo concentration anomaly is assumed to be caused by bonding of Mo to algae-derived organic matter. During the decomposition of deposited organic matter, Mo may be released again leading to significant Mo enrichments in the shallow pore waters.

Besides Mo removal from the water column, Mo concentrations exceeding the salinity-based theoretical values were observed. Laboratory experiments and modelling approaches suggest a significant contribution of resuspended anoxic surface sediments during tidal wave action and storm events on water column Mo budgets due to oxidative release of sulphide-bound Mo. The transfer of isotopically light molybdate, released from degraded organic material or from reoxidised sulphidic sediments, into the water column probably closes the isotope balance between burial of isotopically light Mo adsorbed to aggregates and recycling of light Mo into the water column. The present study shows for the first time the importance of benthic-pelagic coupling for the Mo mass balance in a tidal system based on stable Mo isotope fractionation.

Future work may also focus on the relevance of Mo removal from oxic surface waters and associated Mo isotope fractionation during periods of high productivity in ancient near-coastal systems e.g. during Proterozoic and Mesozoic oceanic anoxic events (OAE) as isotopic pre-fractionation of Mo in oxic surface waters may influence the sedimentary signatures (e. g. Helz et al., 1996; Arnold et al., 2004; Wille et al., 2007). Additionally to the impact of sulphide concentrations (Neubert et al., 2008) as well as metal oxide cycles on the Mo isotopic composition (Reitz et al., 2007), a transfer of isotopically light Mo to the underlying anoxic/sulphidic water body or sediment of a stratified coastal system via sinking aggregates may be assumed.

Acknowledgements

The authors would like to thank A. Resch and K. von Böhlen (RV “Mya”), H. Nicolai and W. Siewert (ICBM-Terramare), M. Groh (Argonauta Wildeshausen), C. Lenz and V. Winde (IOW) for their support during sampling and T. Romanova (AWI Sylt) for the time series sampling and laboratory assistance. We wish to acknowledge D. Benesch, P. Müller, R.

Rosenberg (IOW) for laboratory assistance, and C.-D. Dürselen (AquaEcology, Oldenburg) for phytoplankton counts. Furthermore, we would like to thank R. Asmus (AWI Sylt) for providing the salinity and temperature data from Sylt Site in 2010. We also acknowledge stimulating discussions with B. Flemming, B. Schnetger, and H. Burchard in the initial phase of the study. The associate editor and three anonymous reviewers are thanked for very helpful comments and suggestions. This study was financially supported by the Deutsche Forschungsgemeinschaft (DFG) within the frame of the research group ‘BioGeoChemistry of the Wadden Sea (FOR 432/3) through grants BO 1584/4, BR 775/14-4, and DE 1518/1-1, and the Leibniz IOW. Mo isotope work in Bern was supported by the Deutsche Forschungsgemeinschaft and the Swiss National Science Foundation grant 200020–113658.

References

- Acharya, C., Joseph, D., and Apte, S. K. (2009) Uranium sequestration by a marine cyanobacterium, *Synechococcus elongatus* strain BDU/75042. *Biores. Technol.* 100, 2176-2181.
- Adelson, J. M., Helz, G. R., and Miller, C. V. (2001) Reconstructing the rise of recent coastal anoxia: molybdenum in Chesapeake Bay sediments. *Geochim. Cosmochim. Acta* 65, 237-252.
- Algeo, T. J., Lyons, T. W., Blakey, R. C., and Over, D. J. (2007) Hydrographic conditions of the Devonian-Carboniferous North American seaway inferred from sedimentary Mo-TOC relationships. *Palaeogeogr. Palaeoclimat., Palaeoecol.*, 256, 204-230.
- Allredge, A. L. and Gotschalk, C. C. (1989) Direct observations of mass the flocculation of diatom blooms: characteristics, settling velocities and formation of diatom aggregates. *Deep-Sea Res.* 36, 159-171.
- Aller, R. C., Mackin, J. E., and Cox jr., R. T. (1986). Diagenesis of Fe and S in Amazon inner shelf muds: apparent dominance of Fe reduction and implications for the genesis of ironstones. *Cont. Shelf Res.* 6, 263-289.
- Al-Raei, A. M., Bosselmann, K., Böttcher, M. E., Hespenheide, B., and Tauber, F. (2009). Seasonal dynamics of microbial sulfate reduction in temperate intertidal surface sediments: Controls by temperature and organic matter. *Ocean Dyn.* 59, 351-370.
- Anbar, A. D. and Holland, H. D. (1992). The photochemistry of manganese and the origin of banded iron formation. *Geochim. Cosmochim. Acta* 56, 2595-2603.

541 Armonies, W. and Reise, K. (1999) On the population development of the introduced razor
 542 clam *Ensis americanus* near the island of Sylt (North Sea). Helgol. Meeresunters. 52,
 543 291–300.

544 Arnold, G. L., Anbar, A. D., Barling, J., and Lyons, T. W. (2004) Molybdenum isotope
 545 evidence for widespread anoxia in mid-proterozoic oceans. Science 304, 87-90.

546 Audry, S., Blanc, G., Schäfer, J., Chaillou, G., and Robert, S. (2006) Early diagenesis of trace
 547 metals (Cd, Cu, Co, Ni, U, Mo and V) in the freshwater reaches of a macrotidal estuary.
 548 Geochim. Cosmochim. Acta 70, 2264-2282.

549 Audry, S., Blanc, G., Schäfer, J., and Robert, S. (2007) Effect of estuarine resuspension on
 550 early diagenesis, sulfide oxidation and dissolved molybdenum and uranium distribution
 551 in the Gironde estuary, France. Chem. Geol. 238, 149-167.

552 Barling, J., Arnold, G. L., and Anbar, A. D. (2001) Natural mass-dependent variations in the
 553 isotopic composition of molybdenum. Earth Planet. Sci. Lett. 193, 447-457.

554 Barling, J. and Anbar, A. D. (2004) Molybdenum isotope fractionation during adsorption by
 555 manganese oxides. Earth Planet. Sci. Lett. 217(3-4), 315-329.

556 Bartholomä, A., Kubicki, A., Badewien, T. H., and Flemming, B.W. (2009) Suspended
 557 sediment transport in the German Wadden Sea – seasonal variations and extreme
 558 events. Ocean Dyn. 59(2), 213-226.

559 Bayerl, K., Köster, R., and Murphy, D. (1998) Distribution and composition of sediments in
 560 the List Tidal Basin. In: Gätje, C., Reise, K. (Eds.), The Wadden Sea Ecosystem –
 561 Exchange, Transport and Transformation Processes. Springer, Berlin, Heidelberg, 127-
 562 159.

563 Beck, M., Dellwig, O., Schnetger, B., and Brumsack, H.-J., (2008) Cycling of trace metals
 564 (Mn, Fe, Mo, U, V, Cr) in deep pore waters of intertidal flat sediments. Geochim.
 565 Cosmochim. Acta, 7, 2822-2840.

566 Berrang, P. G. and Grill, E. V. (1974) The effect of manganese oxide scavenging on
 567 molybdenum in Saanich Inlet, British Columbia. Mar. Chem. 2, 125-148.

568 Bhaskar, P. V., Grossart, H.-P., Bhosle, N. B., and Simon, M. (2005) Production of
 569 macroaggregates from dissolved exopolymeric substances (EPS) of bacterial and
 570 diatom origin. FEMS Microb. Ecol. 53, 255-264.

571 Böttcher, M. E., Oelschläger, B., Höpner, T., Brumsack, H.-J., and Rullkötter, J. (1998)
 572 Sulfate reduction related to the early diagenetic degradation of organic matter and
 573 "black spot" formation in tidal sandflats of the German Wadden Sea (southern North

574 Sea): stable isotope (^{13}C , ^{34}S , ^{18}O) and other geochemical results. *Org. Geochem.* 29(5-
575 7) 1517-1530.

576 Böttcher, M. E. (2003) Schwarze Flecken und Flächen im Wattenmeer. In: Lozán, J. L.,
577 Rachor, E., Reise, K., Sündermann, J., Westernhagen, H. V. (eds) Warnsignale aus der
578 Nordsee & Wattenmeer – eine aktuelle Umweltbilanz. Wissenschaftliche
579 Auswertungen, Blackwell, Berlin, pp 193-195.

580 Booij, N., Ris, R. C., and Holthuijsen, L. H. (1999) A third-generation wave model for coastal
581 regions. 1. Model description and validation. *Journal of Geophysical Research* 104,
582 7649-7666.

583 Boudreau, B. P. and Jørgensen, B. B., (Eds.) (2001) The benthic boundary layer – Transport
584 processes and biogeochemistry. Oxford University Press, New York.

585 Burchard, H., and Bolding, K. (2002) GETM a general estuarine transport model. Sci Doc
586 EUR 20253 EN. Institute for Environ and Sustainability, Ispra, Italy.

587 Burdige, D. J., and Nealson, K. H. (1985) Microbial manganese reduction by enrichment
588 cultures from coastal marine sediments. *Appl. Environ. Microbiol.* 50(2), 491-497.

589 Brumsack, H. J. and Gieskes, J. M. (1983) Interstitial water trace-metal chemistry of
590 laminated sediments from the Gulf of California, Mexico. *Marine Chemistry* 14, 89-
591 106.

592 Busch, U., Beckmann, B.-R., and Roth, R. (1998) Study of storm weather situations in
593 observation and ECHAM3/T42 model simulation. *Tellus* 50A, 411-423.

594 Cadée, G.C. (1986) Recurrent and changing seasonal patterns in phytoplankton of the
595 westernmost inlet of the Dutch Wadden Sea from 1969 to 1985. *Mar. Biol.* 93, 281-
596 289.

597 Cantwell, M. G., Burgess, R. M., and Kester, D. R. (2002) Release and phase partitioning of
598 metals from anoxic estuarine sediments during periods of simulated resuspension.
599 *Environ. Sci. Technol.* 36, 5328-5334.

600 Chang, T. S., Bartholomä, A., and Flemming, B. W. (2006) Seasonal dynamics of fine-
601 grained sediments in a back-barrier tidal basin of the German Wadden Sea (Southern
602 North Sea). *J. Coast. Res.* 22(2), 328-338.

603 Christiansen, C., Pejrup, M., Kepp R. R., Nielsen, A., Vølund, G., and Petersen, J. B. T.
604 (2004) Tidal and metrological induced nutrient (N, P) dynamics in the micro-tidal Ho
605 Bugt, Danish Wadden Sea. *Dan. J. Geogr.*, 104, 87-96.

Christiansen, C., Vølund, G., Lund-Hansen, L. C., and Bartholdy, J. (2006) Wind-influence on tidal flat sediment dynamics: Field investigations in the Ho Bugt, Danish Wadden Sea. *Mar. Geol.* 235, 75-86.

Cole, J. J., Lane, J. M., Marino, R., and Howarth, R. W. (1993) Molybdenum assimilation by cyanobacteria and phytoplankton in freshwater and salt water. *Limnol. Oceanogr.* 38(1), 25-35.

Collier, R. W. (1985) Molybdenum in the Northeast Pacific Ocean. *Limnol. Oceanogr.* 30 (6), 1351-1354.

Coveney Jr., R. M., Watney, W. L., and Maples, C. G. (1991) Contrasting depositional models for Pennsylvanian black shale discerned from molybdenum abundances. *Geol.* 19, 147-150.

Daughney, C. J., Fein, J. B., and Yee, N. (1998) A comparison of the thermodynamics of metal adsorption onto two common bacteria. *Chem. Geol.* 144, 161-176.

Davidson, A. T. and Marchant, H. J. (1987) Binding of manganese by Antarctic *Phaeocystis pouchetii* and the role of bacteria in its release. *Mar. Biol.* 95, 481-487.

De Beer, D., Wenzhöfer, F., Ferdelman, T. G., Boehme, S. E., Huettel, M., van Beusekom, J. E., Böttcher, M. E., Musat, N., and Dubilier, N. (2005). Transport and mineralization rates in North Sea sandy intertidal sediments, Sylt-Rømø Basin, Wadden Sea. *Limnol. Oceanogr.* 50(1), 113-127.

De Jonge, V.N. and van Beusekom, J.E.E. (1995) Wind- and tide-induced resuspension of sediment and microphytobenthos from tidal flats in the Ems estuary. *Limnol. Oceanogr.* 40, 766-778.

Dellwig, O., Beck, M., Lemke, A., Lunau, M., Kolditz, K., Schnetger, B., and Brumsack, H.-J., (2007) Non-conservative behaviour of molybdenum in coastal waters: Coupling geochemical, biological, and sedimentological processes. *Geochim. Cosmochim. Acta* 71, 2745-2761.

Dobrynin, M., Gayer, G., Pleskachevsky, A., and Günther, H. (2010) Effect of waves and currents on the dynamics and seasonal variations of suspended particulate matter in the North Sea. *J. Mar. Syst.* 82, 1-20.

Emerson, S., Kalhorn, S., Jacobs, L., Tebo, B. M., Nealson, K. H., and Rosson, R. A. (1982) Environmental oxidation rate of manganese(II): bacterial catalysis. *Geochim. Cosmochim. Acta* 46, 1073-1079.

Erickson, B. E. and Helz, G. R. (2000) Molybdenum(VI) speciation in sulfidic waters: Stability and lability of thiomolybdates. *Geochim. Cosmochim. Acta* 64(7), 1149-1158.

640 Evrard, V., Cook, P.L.M., Veuger, B., Huettel, M., and Middelburg, J.J. (2008) Tracing
641 carbon and nitrogen incorporation and pathways in the microbial community of a photic
642 subtidal sand. *Aquat. Microb. Ecol.* 53, 257-269.

643 Fein, J. B., Martin, A. M., and Wightman, P. G. (2001). Metal adsorption onto bacterial
644 surfaces: Development of a predictive approach. *Geochim. Cosmochim. Acta* 65, 4267-
645 4273.

646 Fein, J. B., Daughney, C. J., Yee, N., and Davis, T. A. (1997) A chemical equilibrium model
647 for metal adsorption onto bacterial surfaces. *Geochim. Cosmochim. Acta* 61, 3319-
648 3328.

649 Fettweis, M., Nechad, B., and van den Eynde, D. (2007) An estimate of the suspended
650 particulate matter (SPM) transport in the southern North Sea using Sea WiFS images, in
651 situ measurements and numeric model results. *Cont. Shelf Res.* 27, 1568-1583.

652 Fettweis, M., Francken, F., van den Eynde, D., Verwaest, T., Janssens, J., and van Lancker,
653 V. (2010) Storm influence on SPM concentrations in a coastal turbidity maximum area
654 with high anthropogenic impact (southern North Sea). *Cont. Shelf Res.* 30, 1417-1427.

655 Flemming, B. W. and Davis jr., R. A. (1994) Holocene evolution, morphodynamics and
656 sedimentology of the Spiekeroog barrier island system (Southern North Sea) *Senckenb.*
657 *marit.* 24(1/6), 117-155.

658 Flemming, B. W. and Nyandwi, N. (1994) Land reclamation as a cause of fine grained
659 sediment depletion in backbarrier tidal flats (Southern North Sea). *Neth. J. Aquat. Ecol.*
660 28, 299-307.

661 Flemming, B. W. and Ziegler, K. (1995) High-resolution grain size distribution patterns and
662 textural trends in the backbarrier environment of Spiekeroog Island (southern North
663 Sea). *Senckenb. Marit.* 26, 1-24.

664 Gätje, Chr. and Reise, K. (Eds.) (1998) *Ökosystem Wattenmeer (The Wadden Sea*
665 *Ecosystem) - Austausch-, Transport- und Stoffumwandlungsprozesse.* Springer Verlag,
666 Berlin, 570 p.

667 Goldberg, T., Archer, C., Vance, D., and Poulton, S. W. (2009) Mo isotope fractionation
668 during adsorption to Fe (oxyhydr)oxides. *Geochim. Cosmochim. Acta* 73, 6502-6516.

669 Goldberg, T., Archer, C., Vance, D., Thamdrup, B., McAnena, A., and Poulton, S.W., (2012)
670 Controls on Mo isotope fractionations in a Mn-rich anoxic marine sediment, Gullmar
671 Fjord, Sweden, *Chemical Geology* 296-297, 73-82.

- Gonçalves, M. L. S., Sigg, L., Reutlinger, M., and Stumm, W. (1987) Metal ion binding by biological surfaces: Voltammetry assessment in the presence of bacteria. *Sci. Total Environ.* 60, 105-119.
- Gräwe, U. and Wolff, J.-O. (2010) Suspended particulate matter dynamics in a particle framework. *Environ Fluid Mech* 10(1-2), 21-39.
- Greber, N. D., Siebert, C., Nögler, T. F., and Pettke, T. (2012) $\delta^{98/95}\text{Mo}$ values and Molybdenum Concentration Data for NIST SRM 610, 612 and 3134: Towards a Common Protocol for Reporting Mo Data. *Geostandards and Geoanalytical Research* 36(3), 291-300.
- Grunwald, M., Dellwig, O., Liebezeit, G., Schnetger, B., Reuter, R., and Brumsack, H.-J. (2007) A novel time-series station in the Wadden Sea (NW Germany): First results on continuous nutrient and methane measurements. *Mar. Chem.* 107, 411-421.
- Grunwald, M., Dellwig, O., Beck, M., Dippner, J. W., Freund, J. A., Kohlmeier, C., Schnetger, B., Brumsack, H.-J. (2009) Methane in the southern North Sea: Sources, spatial distribution and budgets. *Estuar. Coast. Shelf Sci.* 81, 445-456.
- Harvey, R. W. and Leckie, J. O. (1985) Sorption of lead onto two gram-negative marine bacteria in seawater. *Mar. Chem.* 15, 333-344.
- Head, P. C. and Burton, J. D. (1970) Molybdenum in some ocean and estuarine waters. *J. Mar. Biol. Assoc UK Journal* 50, 439-448.
- Heinrichs, H., Brumsack, H.-J., Loftfield, N., and König, N. (1986). Verbessertes Druckaufschlußsystem für biologische und anorganische Materialien. *Zeitschrift für Pflanzenernährung und Bodenkunde* 149, 350-353.
- Helz, G.R., Bura-Nakic, E., Mikac, N., and Ciglenecki, I. (2011) New model for molybdenum behavior in euxinic waters. *Chem. Geol.* 284, 323-332.
- Helz, G. R., Vorlicek, T. P., and Kahn, M. D. (2004) Molybdenum scavenging by iron monosulfides. *Environ. Sci. Technol.* 38, 4263-4268.
- Helz, G. R., Miller, C. V., Charnock, J. M., Mosselmans, J. F. W., Patrick, R. A. D., Garner, C. D., and Vaughan, D. J. (1996) Mechanisms of molybdenum removal from the sea and its concentration in black shales: EXAFS evidence. *Geochim. Cosmochim. Acta* 60, 3631-3642.
- Hillebrand, H., Dürselen, C.-D., Kirschtel, D., Pollinger, U., and Zohary, T. (1999) Biovolume calculation for pelagic and benthic microalgae. *J. Phycol.* 35, 403-424.
- Howarth, R. W., and Cole, J. J. (1985) Molybdenum availability, nitrogen limitation, and phytoplankton growth in natural waters. *Science* 229, 653-655.

706 Huerta-Diaz, M. A. and Morse, J. W. (1992) Pyritization of trace metals in anoxic marine
707 sediments. *Geochim. Cosmochim. Acta* 56, 2681-2702.

708 Jansen, S., Walpersdorf, E., Werner, U., Billerbeck, M., Böttcher, M. E., and de Beer, D.
709 (2009) Functioning of intertidal flats inferred from temporal and spatial dynamics of
710 O₂, H₂S and pH in their surface sediment. *Ocean Dyn.* 59, 317-332.

711 Kalnejais L. H. and Martin W. R. (2007) Role of sediment resuspension in the remobilization
712 of particulate-phase metals from coastal sediments. *Environ. Sci. Technol.* 41, 2282-
713 2288.

714 Kalnejais, L. H., Martin, W. R., and Bothner, M. H. (2010) The release of dissolved nutrients
715 and metals from coastal sediments due to resuspension. *Mar. Chem.* 121, 224-235.

716 Kiørboe, T., Lundsgaard, C., Olesen, M., and Hansen, J. L. S. (1994) Aggregation and
717 sedimentation processes during a spring phytoplankton bloom: A field experiment to
718 test coagulation theory. *J. Mar. Res.* 52, 297-323.

719 Kolditz, K., Dellwig, O., Barkowski, J., Badewien, T. H., Freund, H., and Brumsack, H.-J.
720 (2012) Geochemistry of salt marsh sediments deposited during simulated sea-level rise
721 and consequences for recent and Holocene coastal development of NW Germany. *Geo-*
722 *Mar. Lett.* 32, 42-60.

723 Kowalski, N., Dellwig, O., Beck, M., Grunwald, M., Badewien, T. H., Brumsack, H.-J., van
724 Beusekom, J. E. E., and Böttcher, M. E. (2012) A comparative study of manganese
725 dynamics in the pelagic and benthic parts of two intertidal systems of the North Sea.
726 *Estuar. Coast. Shelf Sci.* 100, 3-17.

727 Kowalski, N., Dellwig, O., Beck, M., Grunwald, M., Fischer, S., Piepho, M., Riedel, T.,
728 Freund, H., Brumsack, H.-J., and Böttcher, M. E. (2009) Trace metal dynamics in the
729 water column and pore waters in a temperate tidal system: response to the fate of algae-
730 derived organic matter. *Ocean Dyn.* 59(2), 333-350.

731 Lavelle, J. W., Mofjeld, H. O., and Baker, E. T. (1984) An in situ erosion rate for a fine-
732 grained marine sediment. *J. Geophys. Res.* 89, 6543-6552.

733 Lemke, A., Lunau, M., Badewien, T. H., and Simon, M. (2010) Short term and seasonal
734 dynamics of bacterial biomass production und amino acid turnover in the water column
735 of an intertidal ecosystem, the Wadden Sea. *Aquat Microb Ecol* 61, 205-218.

736 Lettmann, K. A., Wolff, J.-O., and Badewien, T. H. (2009) Modeling the impact of wind and
737 waves on suspended particulate matter fluxes in the East Frisian Wadden Sea (southern
738 North Sea). *Ocean Dyn.* 59(2), 239-262.

- Logan, B. E., Passow, U., Alldredge, A. L., Grossart, H.-P., and Simon, M. (1995) Rapid formation and sedimentation of large aggregates is predictable from coagulation rates (half-lives) of transparent exopolymer particles (TEP). *Deep-Sea Res. II* 42, 203-214.
- Lübben, A., Dellwig, O., Koch, S., Beck, M., Badewien, T. H., Fischer, S., and Reuter, R. (2009) Distributions and characteristics of dissolved organic matter in temperate coastal waters (Southern North Sea). *Ocean Dyn.* 59, 263-276.
- Lunau, M., Lemke, A., Dellwig, O., and Simon, M. (2006) Physical and biogeochemical controls of microaggregate dynamics in a tidally affected coastal ecosystem. *Limnol. Oceanogr.* 51, 847-859.
- Lund, J. W. G., Kipling, C. and Le Cren, E. D. (1958) The inverted microscope method of estimating algal numbers and the statistical basis of estimations by counting. *Hydrobiol.* 11, 143-170.
- Lyons, T. W., Werne, J. P., Hollander, D. J., Murray, R. W. (2003) Contrasting sulfur geochemistry and Fe/Al and Mo/Al ratios across the last oxic-to-anoxic transition in the Cariaco Bay, Venezuela. *Chem. Geol.* 197, 131-157.
- Marino, R., Howarth, R. W., Chan, F., Cole, J. J., and Likens, G. E. (2003) Sulphate inhibition of molybdenum-independent nitrogen fixation by planktonic cyanobacteria under seawater conditions: a non-reversible effect. *Hydrobiol.* 500, 277-293.
- McManus, J., Nägler, T. F., Siebert, C., Wheat, C. G., Hammond, D. E. (2002) Oceanic molybdenum isotope fractionation: Diagenesis and hydrothermal ridge-flank alteration. *Geochem. Geophys. Geosyst.* 3(12), 1-9.
- Morris, A. W. (1975) Dissolved molybdenum and vanadium in the Northeast Atlantic Ocean. *Deep-Sea Res.* 22 (1), 49-54.
- Morse, J. W. (1994) Interactions of trace metals with authigenic sulfide minerals: implications for the bioavailability. *Mar. Chem.* 46, 1-6.
- Nägler, T. F., Neubert, N., Böttcher, M. E., Dellwig, O. and Schnetger, B. (2011) Mo isotope fractionation in pelagic euxinia: Results from the modern Black and Baltic Seas. *Chem. Geol.* 289, 1-11.
- Nägler, T. F., Siebert, C., Lüschen, H., and Böttcher, M. E. (2005) Sedimentary Mo isotope record across the Holocene fresh-brackish water transition of the Black Sea. *Chem. Geol.* 219, 283-295.
- Neubert, N., Heri, A. R., Voegelin, A. R., Nägler, T. F., Schlunegger, F., and Villa, I. M. (2011) The molybdenum isotopic composition in river water: Constraints from small catchments. *Earth Planet. Sci. Lett.* 304, 180-190.

773 Neubert, N., Nögler, T., and Böttcher, M.E. (2008) Sulfidity controls molybdenum isotope
774 discrimination into euxinic sediments: Evidence from the modern Black Sea. *Geology*
775 36, 775-778.

776 Nico, P. S., Anastasio, C., Zasoski, R. J. (2002) Rapid photo-oxidation of Mn(II) mediated by
777 humic substances. *Geochim. Cosmochim. Acta* 66, 4047-4056.

778 Nissenbaum, A. and Swaine, D. J. (1975) Organic matter-metal interactions in recent
779 sediments: the role of humic substances. *Geochim. Cosmochim. Acta* 40, 809-816.

780 Passow, U. (2002a) Transparent exopolymer particles (TEP) in aquatic environments. *Progr.*
781 *Oceanogr.* 55(3-4), 287-333.

782 Passow, U. (2002b) Production of transparent exopolymer particles (TEP) by phyto- and
783 bacterioplankton. *Mar Ecol Prog Ser* 236, 1-12.

784 Postma, H. (1961) Transport and accumulation of suspended matter in the Dutch Wadden
785 Sea. *Neth. J. Sea Res.* 1, 148-190.

786 Poulson, R. L., Siebert, C. McManus, J., and Berelson, W. M. (2006) Authigenic
787 molybdenum isotope signatures in marine sediments. *Geology* 34, 617-620.

788 Reineck, H.-E., Chen, C., Wang, S. (1986) Die Rückseitenwatten zwischen Wangerooge und
789 Festland, Nordsee. *Senckenb. Marit.* 17, 241-252.

790 Reitz, A., Wille, M., Nögler, Th. F., and de Lange G. J. (2007) Atypical Mo isotope signatures
791 in eastern Mediterranean sediments. *Chemical Geology* 245, 1-8.

792 Riebesell, U. (1991a) Particle aggregation during a diatom bloom. I. Physical aspects. *Mar.*
793 *Ecol. Progr. Ser.* 69, 273-280.

794 Riebesell, U. (1991b) Particle aggregation during a diatom bloom. II. Biological aspects. *Mar.*
795 *Ecol. Progr. Ser.* 69, 281-291.

796 Roman, M. R. and Tenore, K. R. (1978) Tidal resuspension in Buzzards Bay,
797 Massachusetts. *Estuar. Coast. Mar. Sci.* 6, 37-46.

798 Rusch, A. and Huettel, M. (2000) Advective particle transport into permeable sediments –
799 evidence from experiments in an intertidal sandflat. *Limnol. Oceanogr.* 45(3), 524-533.

800 Saulnier, I. and Mucci, A. (2000) Trace metal remobilization following the resuspension of
801 estuarine sediments: Saguenay Fjord, Canada. *Appl. Geochem.* 15, 191-210.

802 Schoemann, V., Becquevort, S., Stefels, J., Rousseau, V., and Lancelot, C. (2005) Phaeocystis
803 blooms in the global ocean and their controlling mechanisms: a review. *J. Sea Res.* 53,
804 43-66.

805 Seders, L. and Fein, J. B. (2011) Proton binding of bacterial exudates determined through
806 potentiometric titrations. *Chem. Geol.* 285, 115-123.

- 807 Siebert, C., Nögler, T. F., von Blanckenburg, F., and Kramers, J. D. (2003) Molybdenum
808 isotope records as a potential new proxy for paleoceanography. *Earth Planet. Sci. Lett.*
809 211, 159-171.
- 810 Siebert, C., Nögler, T.F., and Kramers, J.D. (2001) Determination of molybdenum isotope
811 fractionation by double-spike multicollector inductively coupled plasma mass
812 spectrometry. *Geochem. Geophys. Geosyst.* 2: Nil_1-Nil_16.
- 813 Simon, M., Grossart, H.-P., Schweitzer, B., and Ploug, H. (2002) Microbial ecology of
814 organic aggregates in aquatic ecosystems. *Aquat. Microb. Ecol.* 28, 175-211.
- 815 Stanev, E. V., Wolff, J.-O., and Brink-Spalink, G. (2006) On the sensitivity of the
816 sedimentary system in the East Frisian Wadden Sea to sea level rise and wave-induced
817 bed shear stress. *Ocean Dyn.* 56, 266-283.
- 818 Sterckx, S., Knaeps, E., Bollen, M., Trouw, K., and Houthuys, R. (2007) Retrieval of
819 suspended sediment from advanced hydrospectral sensor data in the Scheldt estuary at
820 different stages in the tidal cycle. *Mar. Geodesy* 30, 97-108.
- 821 Streif, H. (1990) Das ostfriesische Küstengebiet – Nordsee, Inseln, Watten und Marschen.
822 Sammlung Geologischer Führer, 2. völlig Neubearb. Aufl., Gebrüder Borntraeger,
823 Berlin, Stuttgart, 376 p.
- 824 Szilagyi, M. (1967). Sorption of molybdenum by humus preparations. *Geochem. Int.* 4, 1165-
825 1167.
- 826 Tilch, E. (2003) Oszillation von Wattflächen und deren fossiles Erhaltungspotential
827 (Spiekerooger Rückseitenwatt, südliche Nordsee). Berichte, Fachbereich
828 Geowissenschaften, Universität Bremen, Nr. 222, 137 Seiten, Bremen.
- 829 Tuit, C. B., Ravizza, G. (2003) The marine distribution of molybdenum. *Geochim.*
830 *Cosmochim. Acta* 67(18), A495-A495 Suppl. 1.
- 831 UNESCO (1985) The international system of units (SI) in oceanography. *Techn. Papers Mar.*
832 *Sci.* 45, 124 pp.
- 833 Utermöhl, von H. (1931) Neue Wege in der quantitativen Erfassung des Planktons. (Mit
834 besonderer Berücksichtigung des Ultraplanktons). *Verh. Int. Ver. Theor. Angew.*
835 *Limnol.* 5, 567-595.
- 836 Van Beusekom, J.E.E., Loebl, M., and Martens, P. (2009) Distant riverine nutrient supply and
837 local temperature drive the long-term phytoplankton development in a temperate coastal
838 basin. *J. Sea Res.* 61, 26-33.
- 839 Volkenborn, N., Hedtkamp, S. I. C., van Beusekom, J. E. E., and Reise, K. (2007) Effects of
840 bioturbation and bioirrigation by lugworms (*Arenicola marina*) on physical and

841 chemical sediment properties and implications for intertidal habitat succession. *Estuar.*
842 *Coast. Shelf Sci.* 74, 331-343.

843 Vorliceck, T. P., Kahn, M. D., Kasuya, Y., and Helz, G. R. (2004) Capture of molybdenum in
844 pyrite-forming sediments: Role of ligand-induced reduction by polysulfides. *Geochim.*
845 *Cosmochim. Acta* 68(3), 547-556.

846 Walther, F. (1972) Zusammenhänge zwischen der Größe der ostfriesischen Seegatten mit
847 ihren Wattgebieten sowie Watten und Strömungen. Jahresbericht 1971. Forschungsstelle
848 für Insel- und Küstenschutz, Norderney.

849 Warner, J. C., Butman, B., and Dalyander, P. S. (2008) Storm-driven sediment transport in
850 Massachusetts Bay. *Cont. Shelf Res.* 28, 257-282.

851 Wasylenki, L. E., Rolfe, B., A., Weeks, C. L., Spiro, T. G., and Anbar, A. D. (2008)
852 Experimental investigation of the effects of temperature and ionic strength on Mo
853 isotope fractionation during adsorption to manganese oxides. *Geochim. Cosmochim.*
854 *Acta* 72, 5997-6005.

855 Wille, M., Kramers, J. D., Nögler, T. F., Beukes, N., Schröder, S., Meisel, T., Lacassie, J. P.,
856 and Voegelin, A. R. (2007) Evidence for a gradual rise of oxygen between 2.6 and 2.5
857 Ga from Mo isotopes and Re-PGE signatures in shales. *Geochim. Cosmochim. Acta* 71,
858 2417-2435.

859 Xue, H.-B., Stumm, W., and Sigg, L. (1988) Binding of heavy metal to algal surfaces. *Water*
860 *Res.* 22, 917-926.

861 Yamazaki, H., Gohda, S. (1990) Distribution of Dissolved Molybdenum in the Seto Inland
862 Sea, the Japan Sea, the Bering Sea and the Northwest Pacific-Ocean. *Geochem. J.*
863 24(4), 273-281.

864 You, Z.-J. (2005) Fine sediment resuspension dynamics in a large semi-enclosed bay. *Ocean*
865 *Engineering* 32, 1982-1993.

866 Zerkle, A. L., Scheiderich, K., Mareska, J. A., Liermann, L. J., and Brantley, S. L. (2011)
867 Molybdenum isotope fractionation by cyanobacterial assimilation during nitrate
868 utilization and N₂ fixation. *Geobiol.* 9, 94-106.

Table 1: Mo concentrations/contents and isotopic composition in the water column, SPM, and sediments at Spiekeroog Site and of biota collected from different sites. Uncertainties of $\delta^{98/95}$ Mo represent run precisions. External reproducibility is +/- 0.06 (2s).

Sample	$\delta^{98/95}\text{Mo}$	2σ	Mo [nM]
Water column			
29 Apr 2008	2.23	0.05	110
16 June 2008	2.52	0.04	60
24 June 2008	2.45	0.05	50
11 Aug 2008	2.37	0.05	90
23 Sept 2008	2.25	0.06	100
28 June 2007	-	-	70
19 July 2007	-	-	130
4 Sept 2007	-	-	90
SPM			
28 June 2007	0.28	0.03	0.60
19 July 2007	0.93	0.06	0.31
4 Sept 2007	1.09	0.05	1.07
Sediment			mg kg⁻¹
<i>Janssand July 2006:</i>			
Oxic surface: 0.8-1.0 cmbsf	0.34		0.10
8.0-10.5 cmbsf	0.56		0.12
Anoxic surface: 0-1.0 cmbsf	0.79		0.16
9.0-10.5 cmbsf	0.89		0.12
<i>27 Mar 2008: (used for experiments)</i>			
Anoxic sandy sediment (JS)	0.46	0.06	0.44
Anoxic mixed sediment (NN)	1.45	0.03	1.31
Periostraca			mg kg⁻¹
<i>Mytilus edulis</i>	-	-	8

Ensis americanus

Sylt June 2009	-	-	118
----------------	---	---	-----

Ensis americanus

Sylt Nov 2009	-	-	256
---------------	---	---	-----

Ensis americanus

Norderney Jan 2010	1.29		160
--------------------	------	--	-----

Figure captions

Fig. 1: Map of the study areas in the German Wadden Sea;

A) Backbarrier area of Spiekeroog Island with sampling sites for seawater (OB, time series station) and sediments (Janssand, JS, Neuharlingersieler Nacken, NN).

B) Sylt-Rømø tidal basin (Sylt Island) with sampling site LL.

Fig. 2: Time series of a) dissolved molybdenum (open circles: measured values; black circles: calculated from salinity, black arrows indicate the most prominent positive concentration anomalies) and manganese (grey circles), b) water temperature and cell carbon of diatoms (open squares) and *Phaeocystis sp.* (black squares) in the water column of the backbarrier area of Spiekeroog Island. The grey line marks the usual seawater value of Mo.

Fig. 3: Time series of a) dissolved molybdenum (open circles: measured values; black circles: calculated from salinity, black arrows mark the most prominent positive concentration anomalies) and manganese (grey circles), b) water temperature and cell carbon of diatoms (open squares) and *Phaeocystis sp.* (black squares) in the water column of the Sylt-Rømø tidal basin. The black arrow indicates a further increase of cell carbon in March 2010 up to 1202 $\mu\text{g L}^{-1}$. The grey line marks the usual seawater value of Mo.

Fig. 4: a) Mo_{diss} concentrations (black circles) in the water column of Site Spiekeroog (OB) during the depletion period in 2008 with corresponding $\delta^{98/95}\text{Mo}$ values (open circles). The grey line marks the mean ocean molybdenum value (MOMo). Error bars indicate measurement uncertainties. b) Scatterplot of Mo_{diss} and $\delta^{98/95}\text{Mo}$ showing a distinct negative correlation of $r = -0.94$. The grey circle denotes the MOMo.

Fig. 5: Estimation of Mo isotope fractionation with a calculated enrichment factor using a Rayleigh-based equation and comparison with factors determined during Mo scavenging by Mn oxides (*Wasylenki et al., 2008) and FeOOH (**Goldberg et al., 2009) and by biological Mo uptake (**Zerkle et al., 2011).

Fig. 6: a) Wind speed (*open circles*) and SPM concentrations (*black circles*) in the backbarrier area of Spiekeroog Island in August 2003.

b) Anoxic surface sediments are suspended in the main tidal channel at the eastern margin of the Jansand flat after a change from an eastern to a north-western wind regime (spring 2006; photo: M.E. Böttcher). The black colour (*arrows*) is caused by resuspension of iron monosulphide-rich sediment material.

Fig. 7: Oxidation experiment with natural anoxic sand flat (*grey open circles*) and mixed flat (*black circles*) sediments suspended in oxygenated artificial seawater; a) concentration of dissolved Mo versus the time of the experiment; b) calculated rates of Mo release from the sediments during oxidation; c) Isotopic composition of the released Mo_{diss} .

Fig. 8: Model-derived residence times of suspended particles (grain size diameter 50 μm) in the water column of the backbarrier area of Spiekeroog Island a) during calm weather conditions, and b) during the storm event “Britta” (November 2006). Figure c) presents a difference map (b minus a).

Fig. 9: Generalised illustration of the benthic-pelagic interactions influencing the Mo cycle in a tidal system.

Figure 1
[Click here to download high resolution image](#)

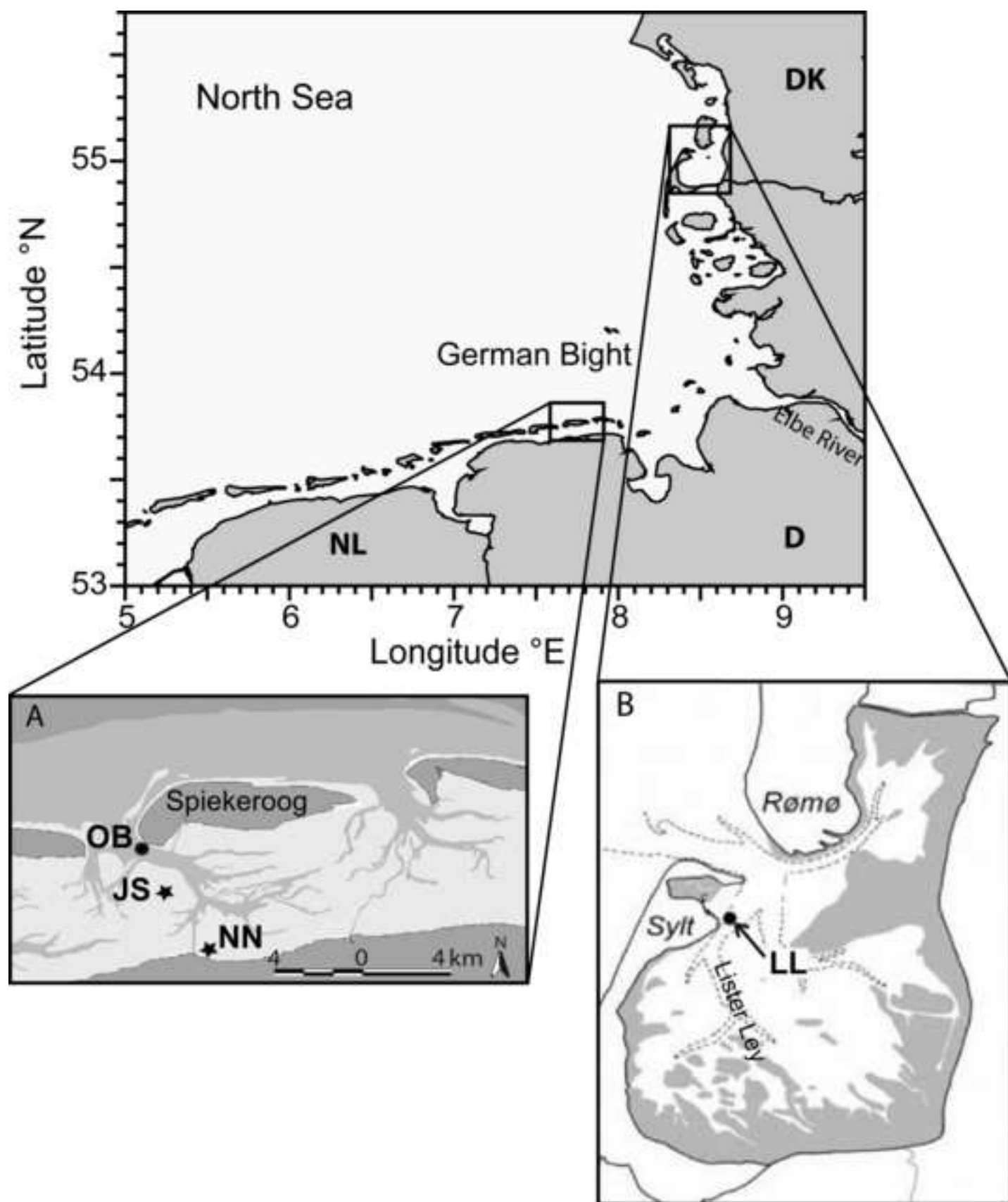


Fig. 1_NK

Figure 2
[Click here to download high resolution image](#)

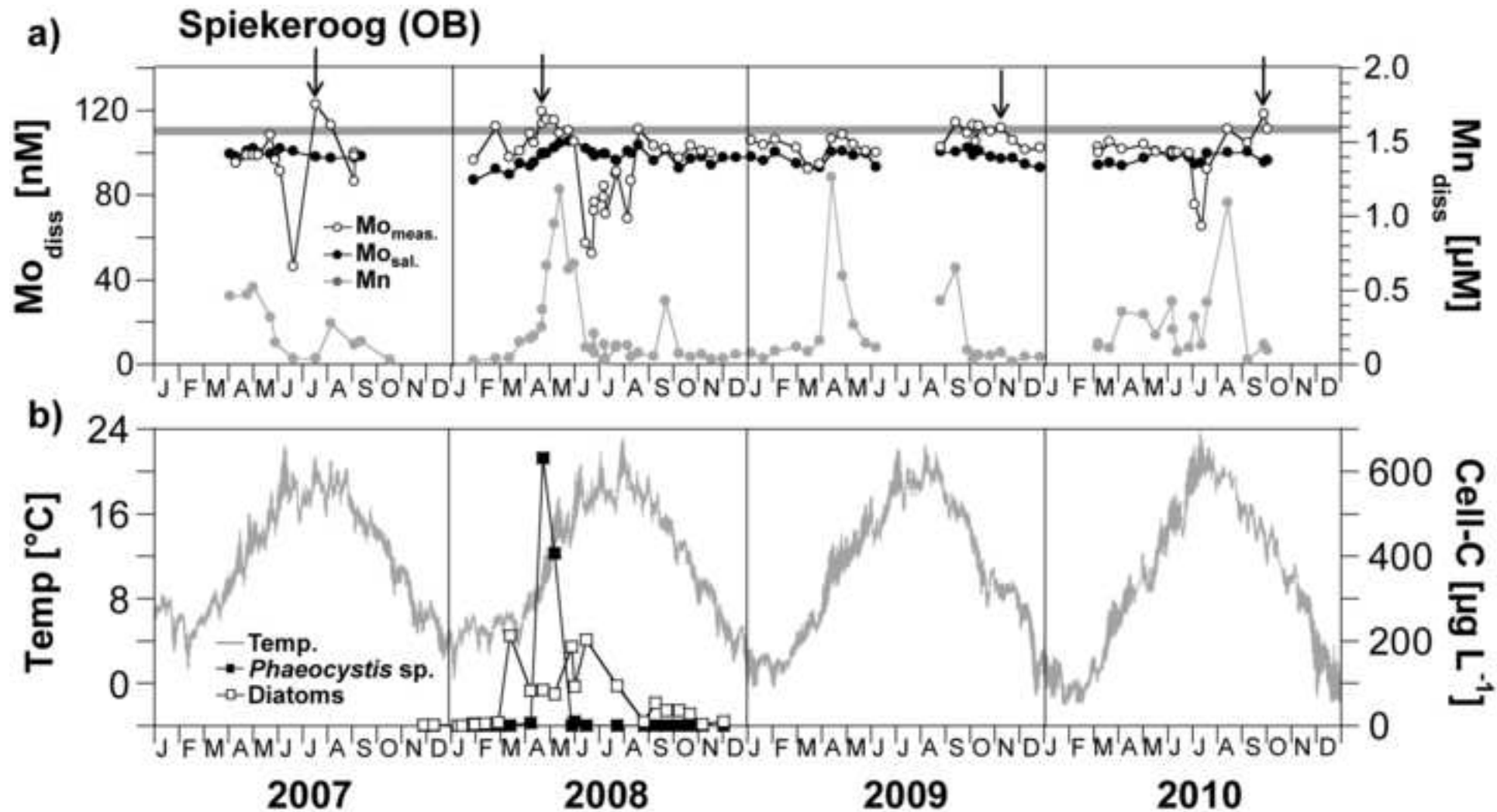


Fig. 2_NK

Figure 3
[Click here to download high resolution image](#)

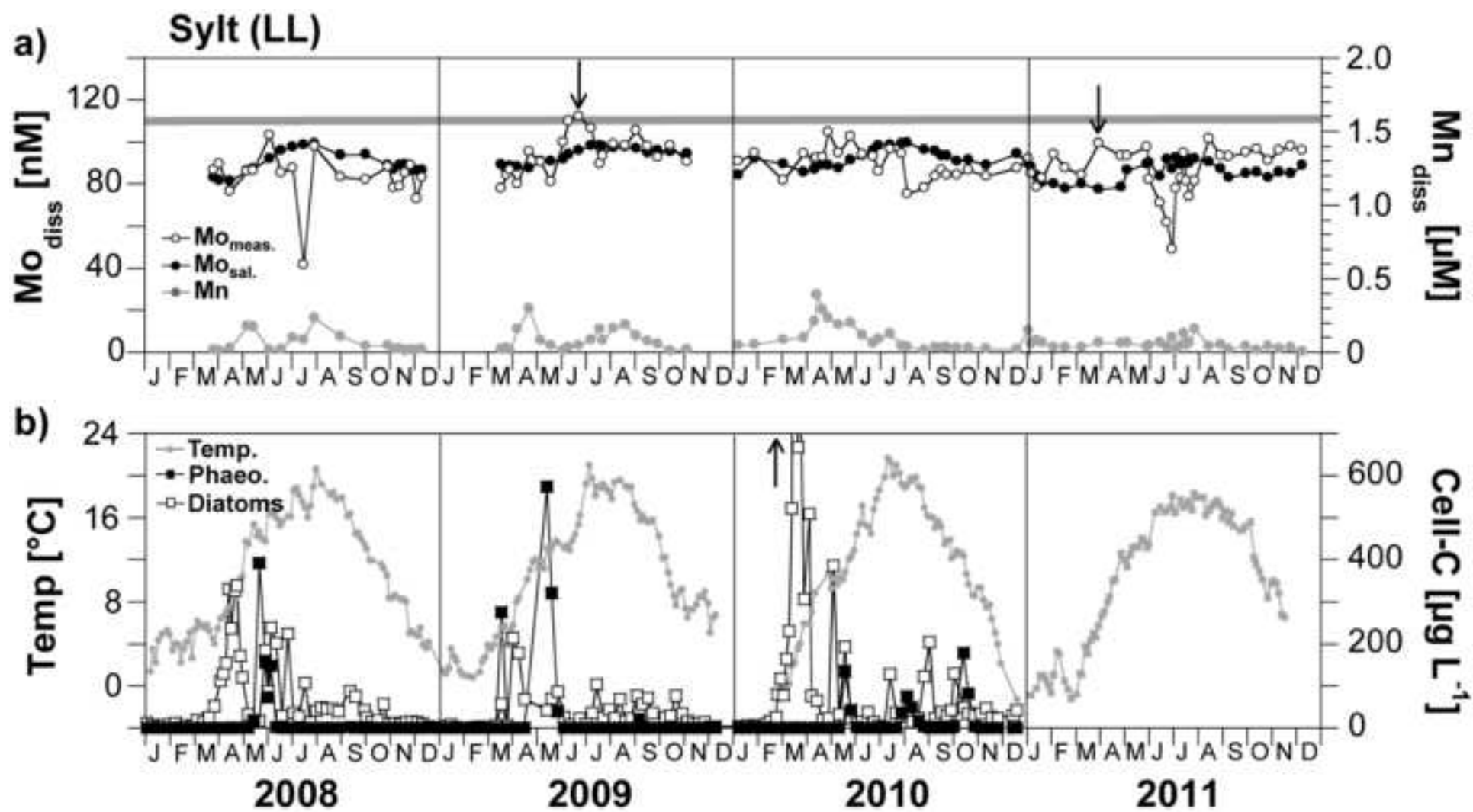


Fig. 3_NK

Figure 4
[Click here to download high resolution image](#)

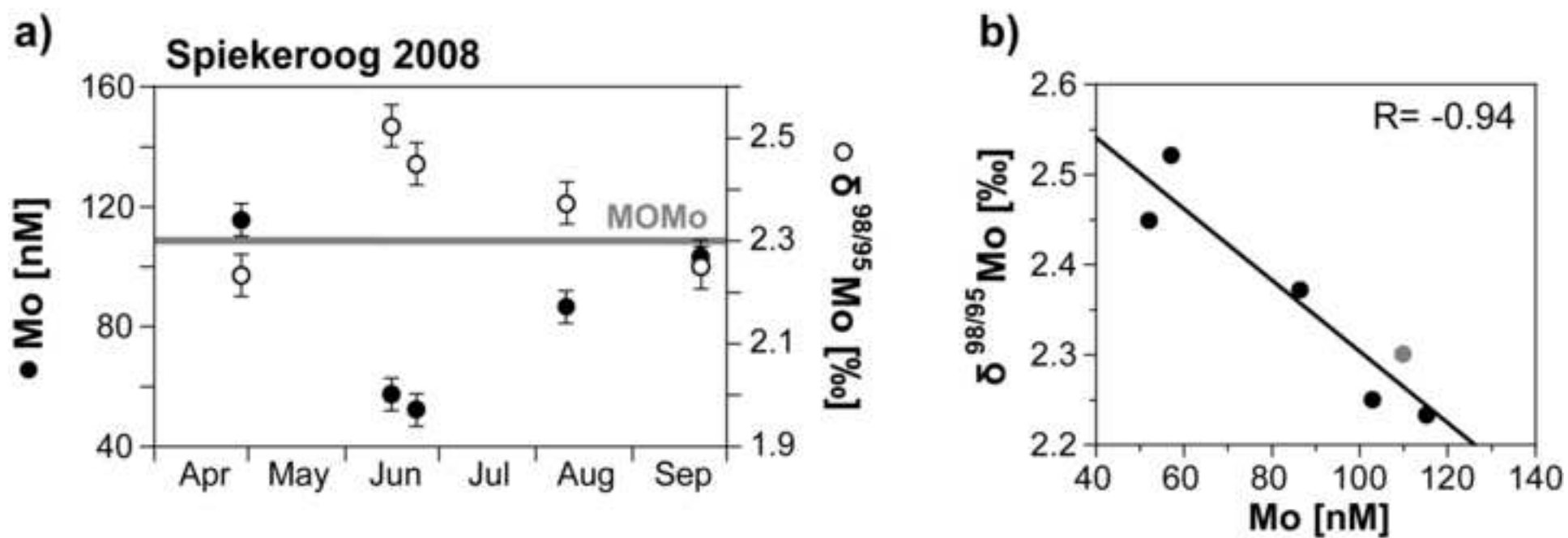


Fig. 4_NK

Figure 5
[Click here to download high resolution image](#)

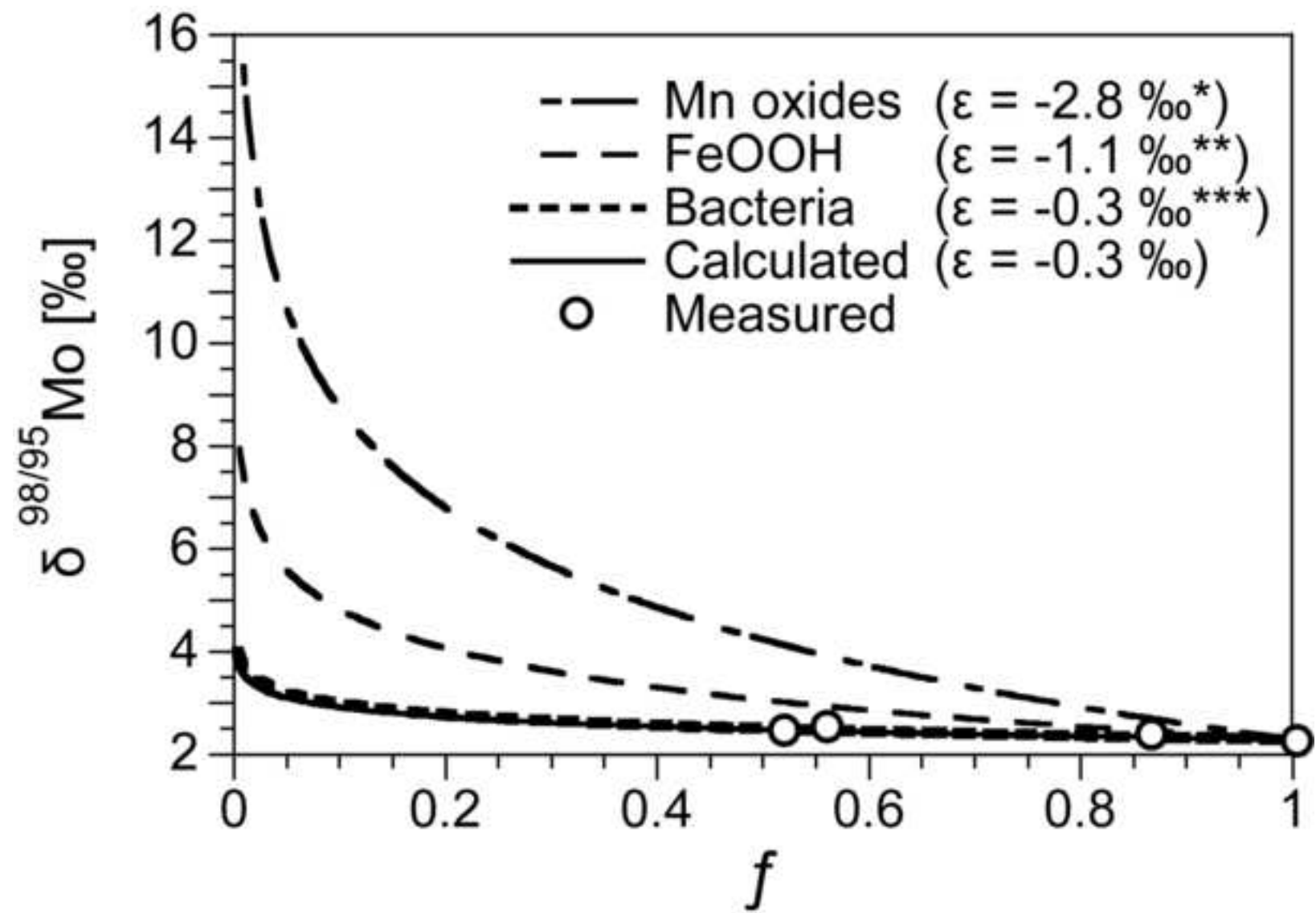


Fig. 5_NK

Figure 6
[Click here to download high resolution image](#)

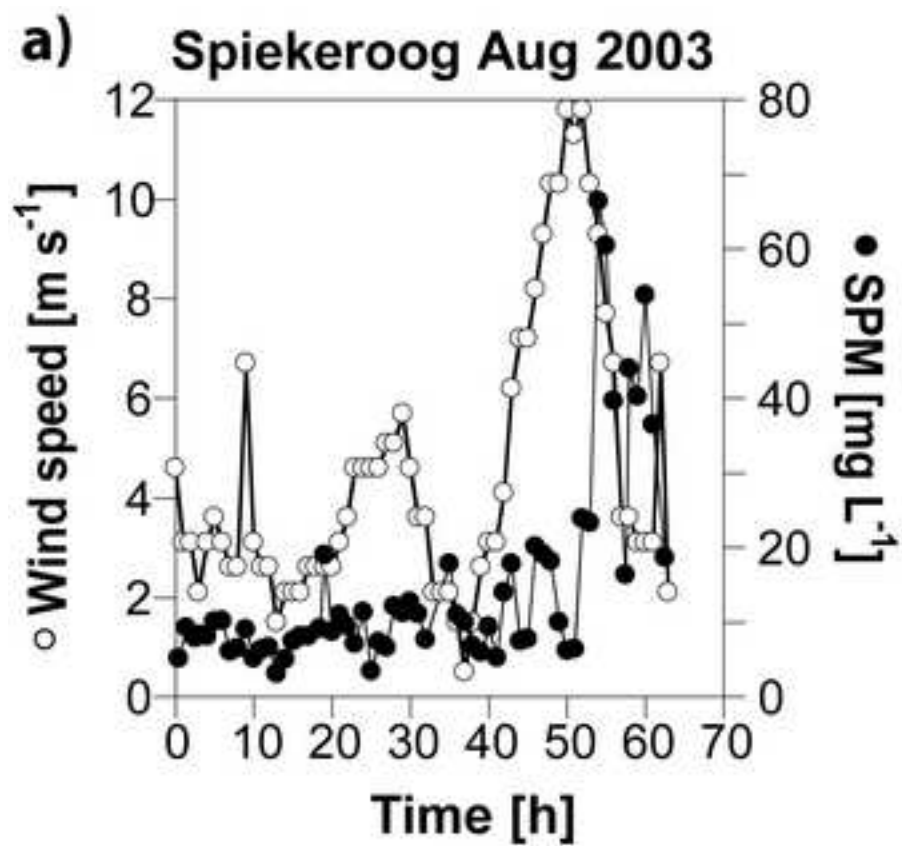


Fig. 6_NK

Figure 7
[Click here to download high resolution image](#)

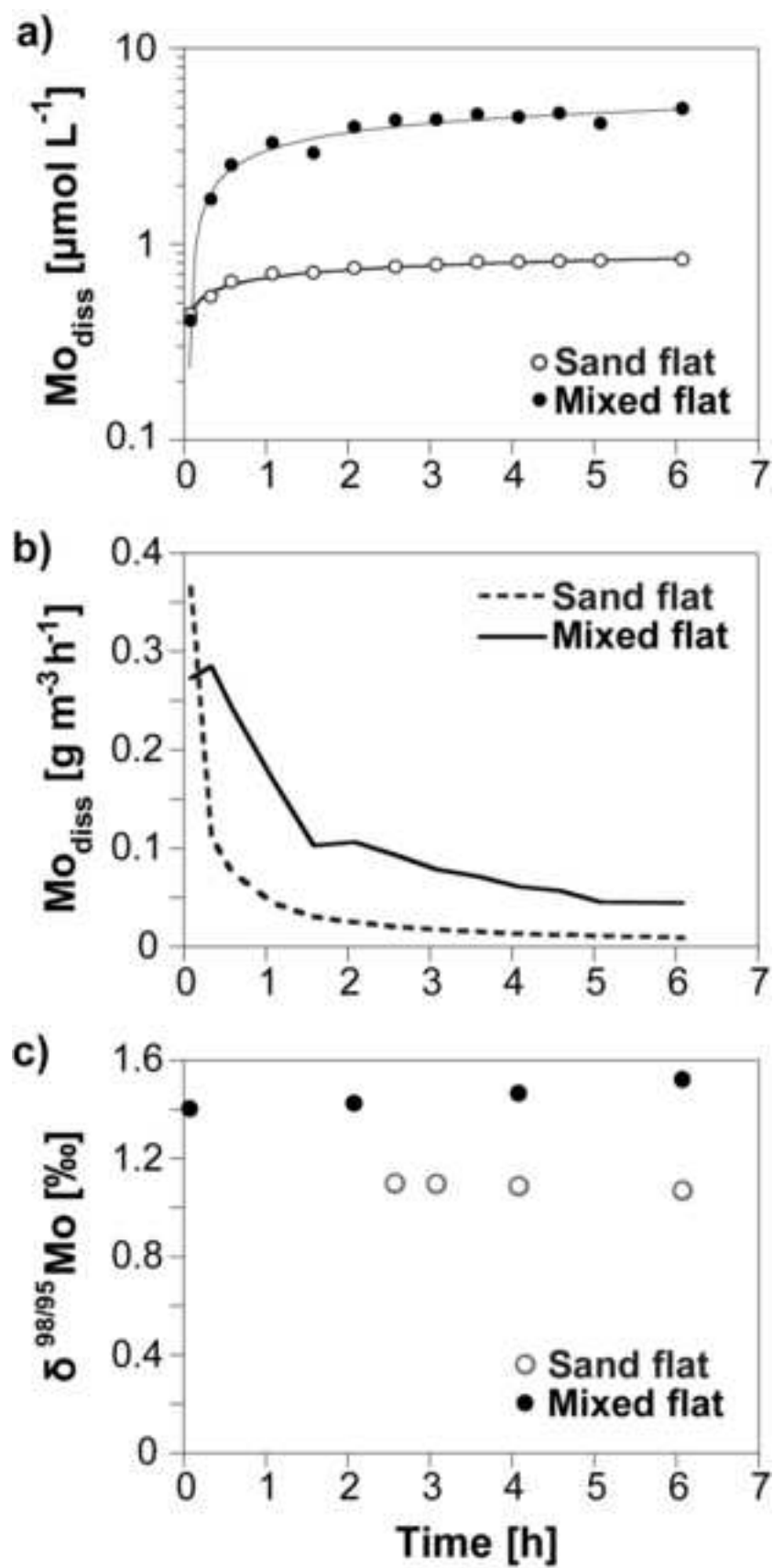


Fig. 7_NK

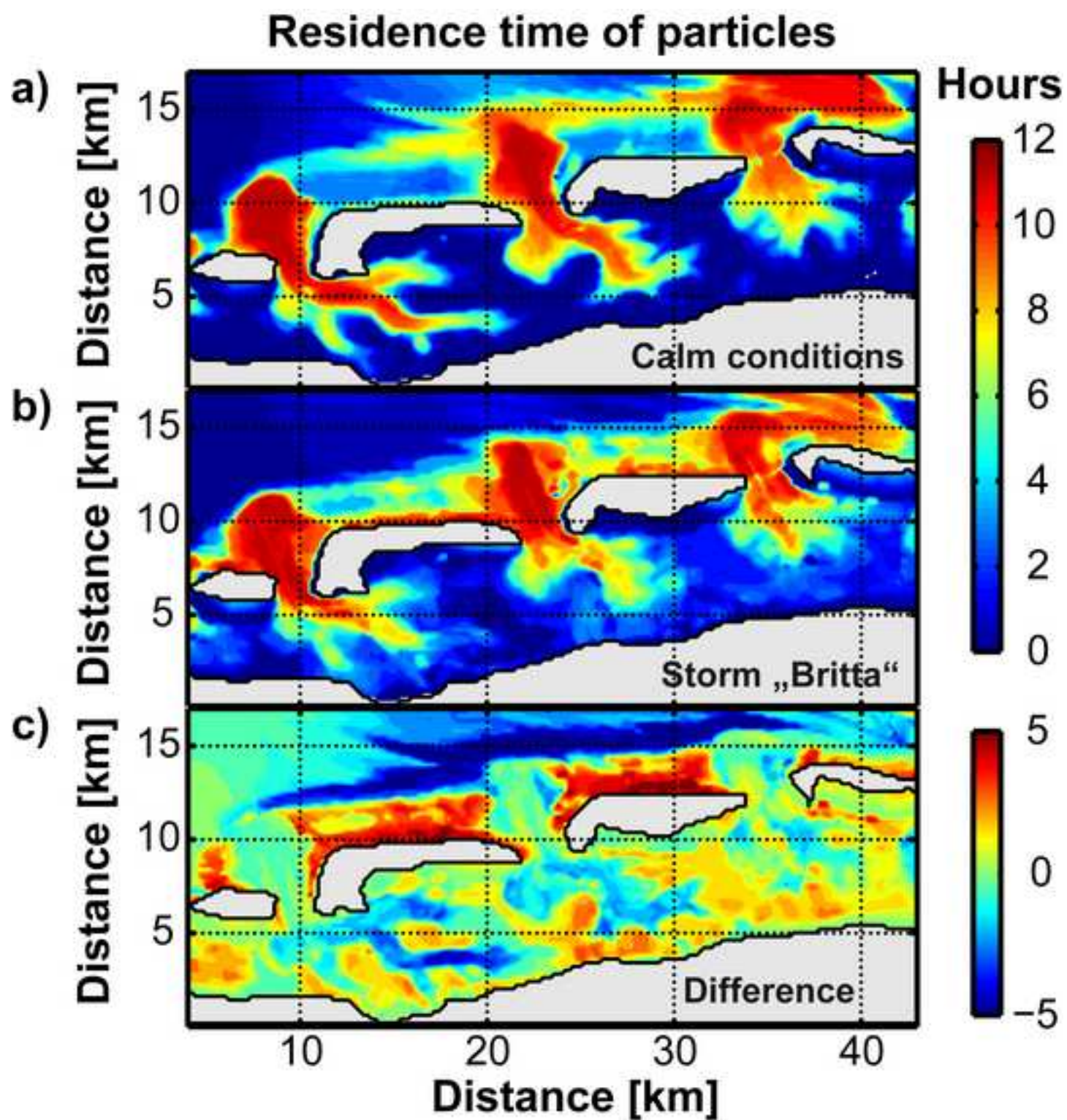


Fig. 8_NK

Figure 9
[Click here to download high resolution image](#)

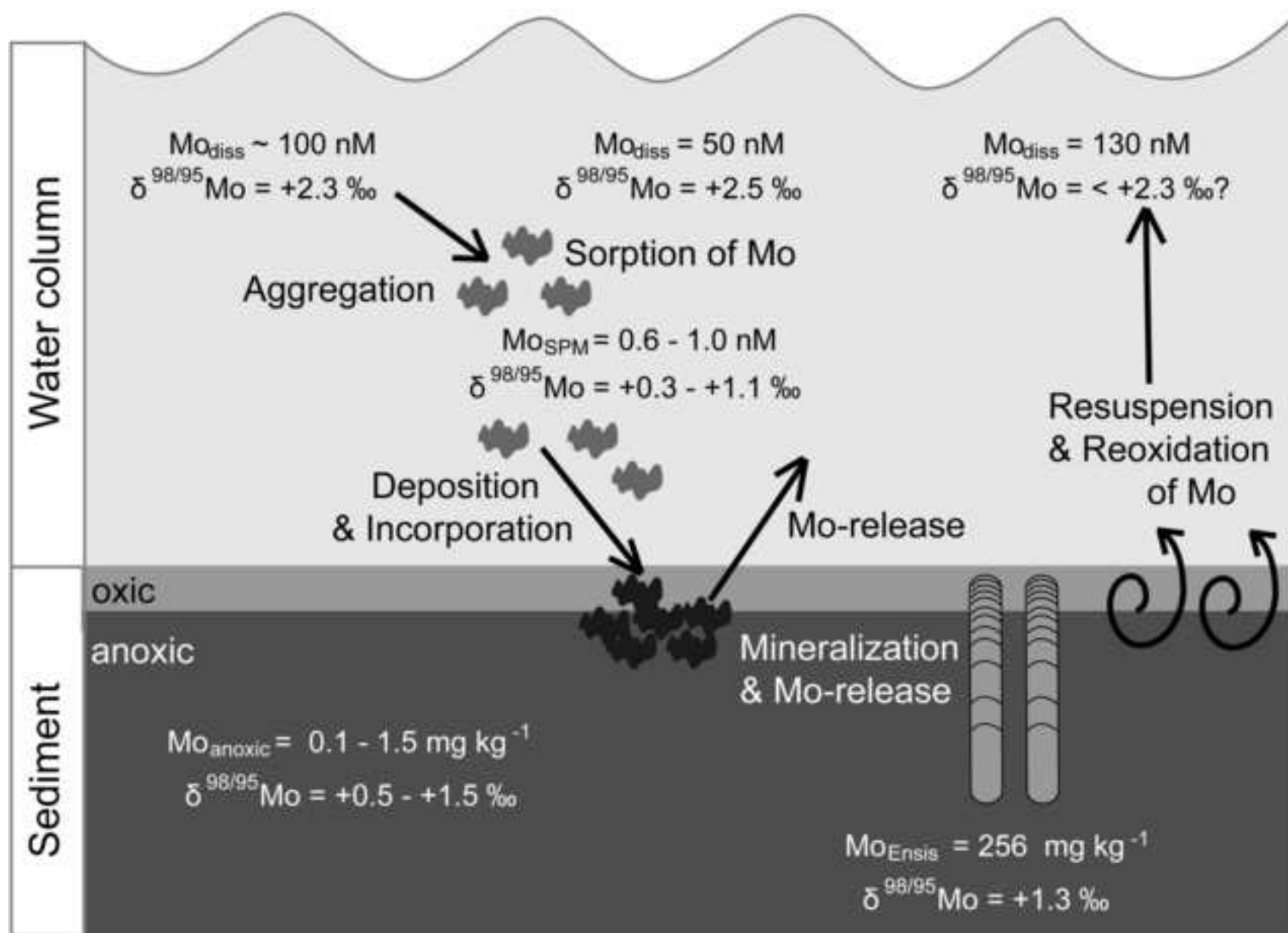


Fig. 9_NK